

# Measurement of ridge and $v_2$ in 13 and 2.76 TeV $pp$ collisions with ATLAS

**Mingliang Zhou**

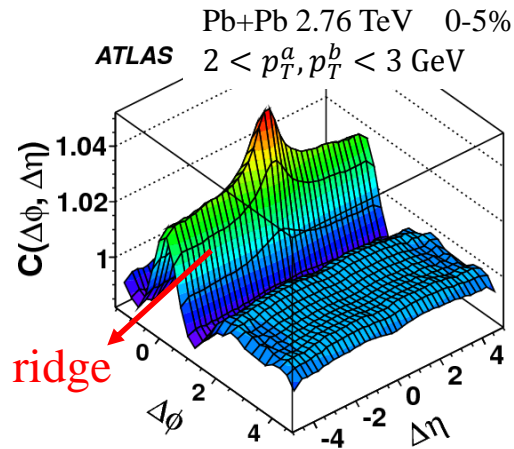
for the ATLAS collaboration

Sep 29<sup>th</sup> , 2015

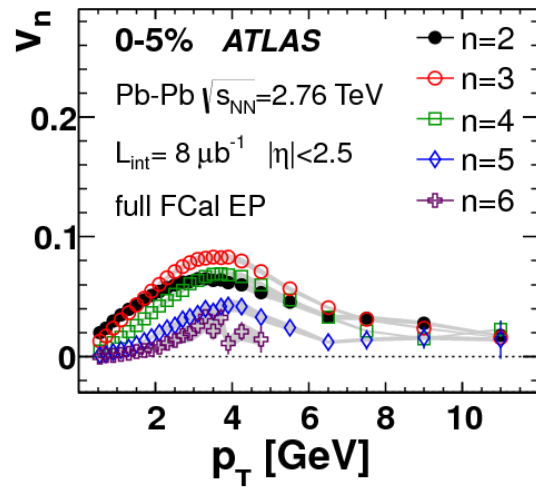
<http://arxiv.org/abs/1509.04776>



# Introduction

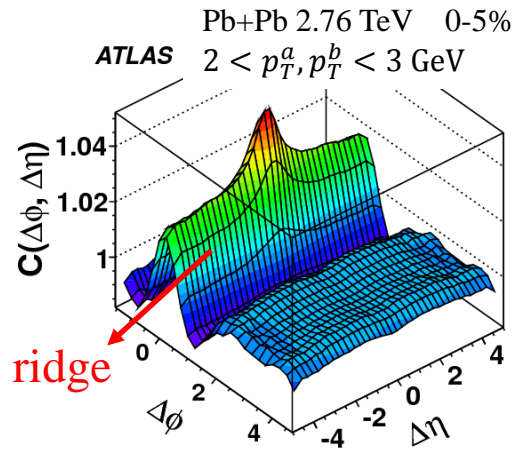


The ridge first discovered in A+A collisions.

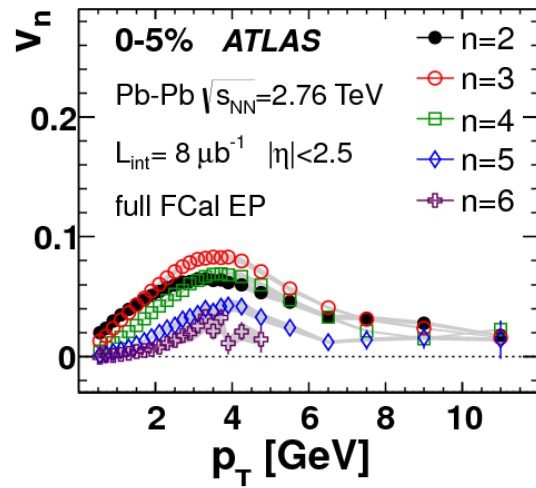


Single-particle  $v_n$  was measured.

# Introduction

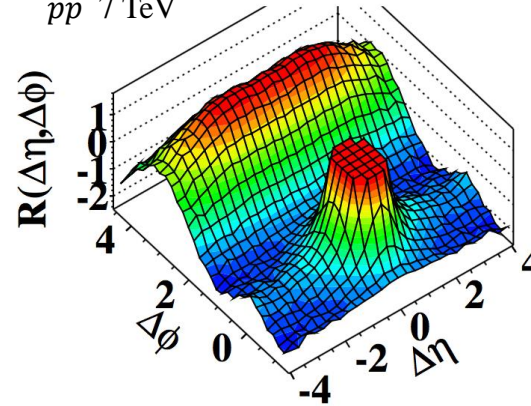


The ridge first discovered in A+A collisions.



Single-particle  $v_n$  was measured.

**CMS**  $N \geq 110, 1.0 \text{ GeV}/c < p_T < 3.0 \text{ GeV}/c$   
 $pp$  7 TeV

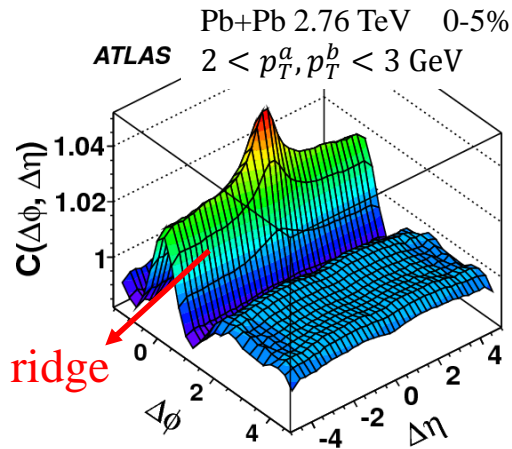


Ridge observed in  $pp$ .

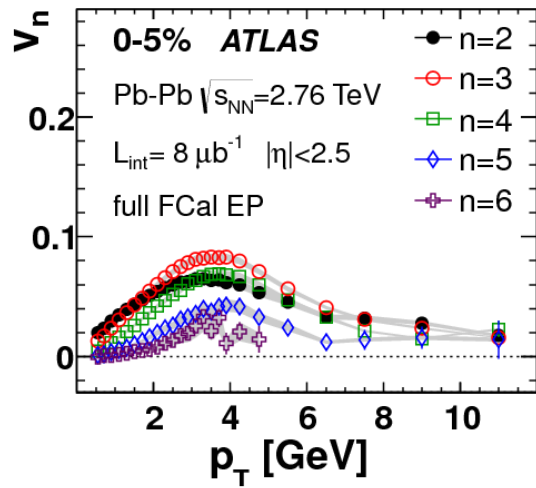
Theoretical interpretations

- Flow effects?
- Initial state physics?

# Introduction

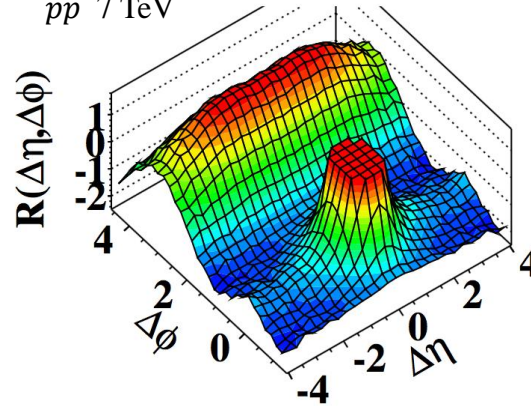


The ridge first discovered in A+A collisions.



Single-particle  $v_n$  was measured.

**CMS**  $N \geq 110, 1.0 \text{ GeV}/c < p_T < 3.0 \text{ GeV}/c$   
 $pp$  7 TeV

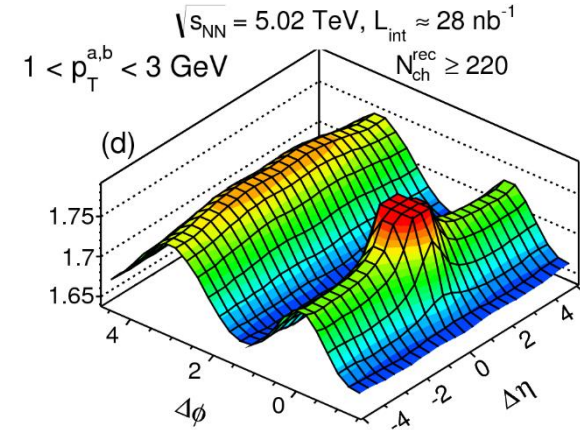


Ridge observed in pp.

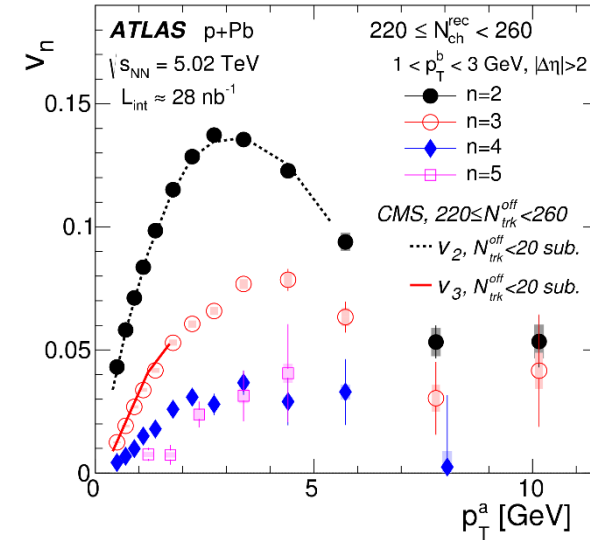
Theoretical interpretations

- Flow effects?
- Initial state physics?

**ATLAS** p+Pb

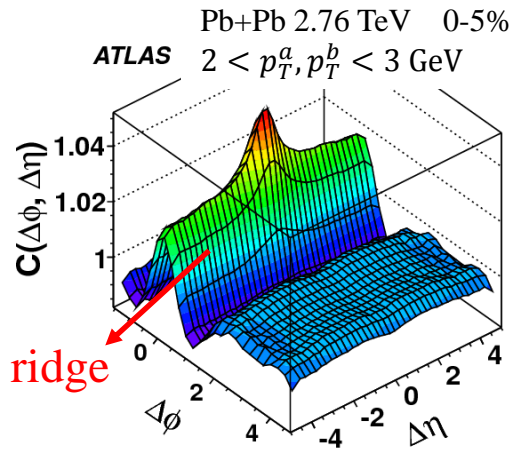


Ridge in p+Pb.

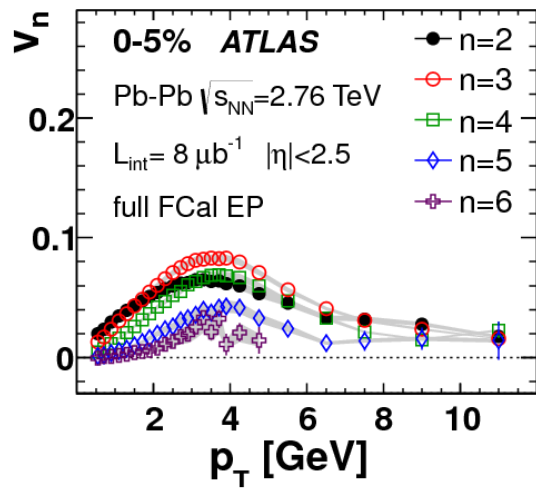


$v_n$  was also measured.

# Introduction

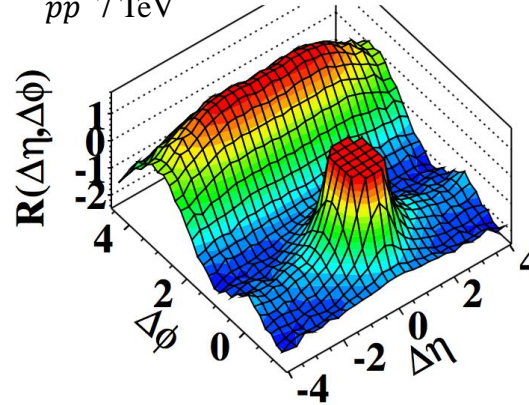


The ridge first discovered in A+A collisions.



Single-particle  $v_n$  was measured.

**CMS**  $N \geq 110, 1.0 \text{ GeV}/c < p_T < 3.0 \text{ GeV}/c$   
 $pp$  7 TeV



Ridge observed in  $pp$ .

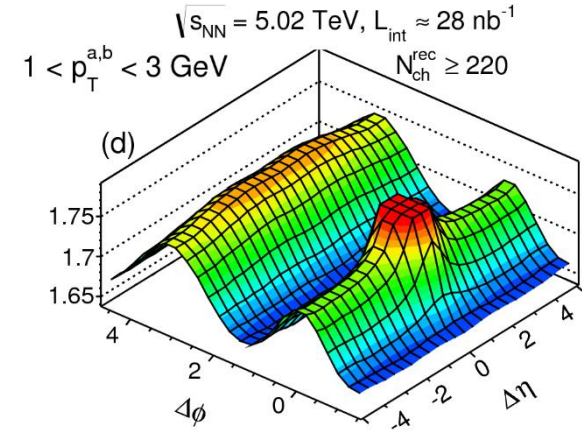
Theoretical interpretations

- Flow effects?
- Initial state physics?

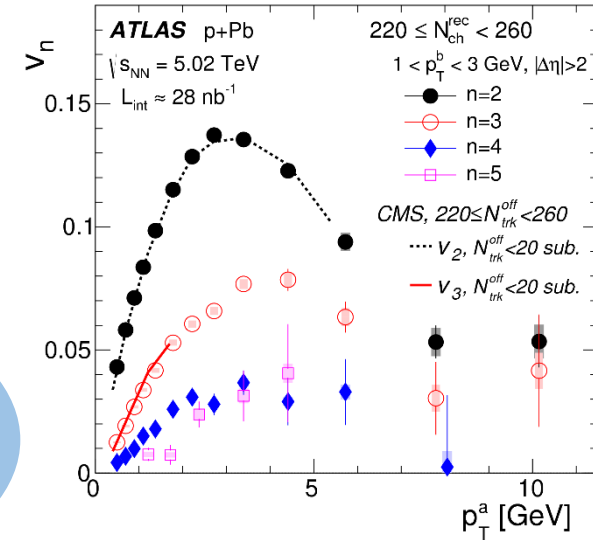
To shed light on competing theories, more studies needed:

- Single-particle  $v_n$ ;
- Energy dependence.

**ATLAS** p+Pb



Ridge in p+Pb.



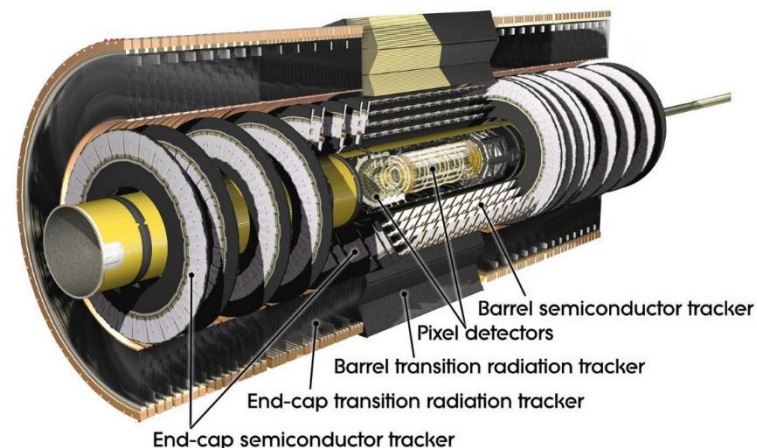
$v_n$  was also measured.

# Data set

- ATLAS  $pp$  2.76 and 13 TeV data
- Charge particle tracks reconstructed in Inner Detector:

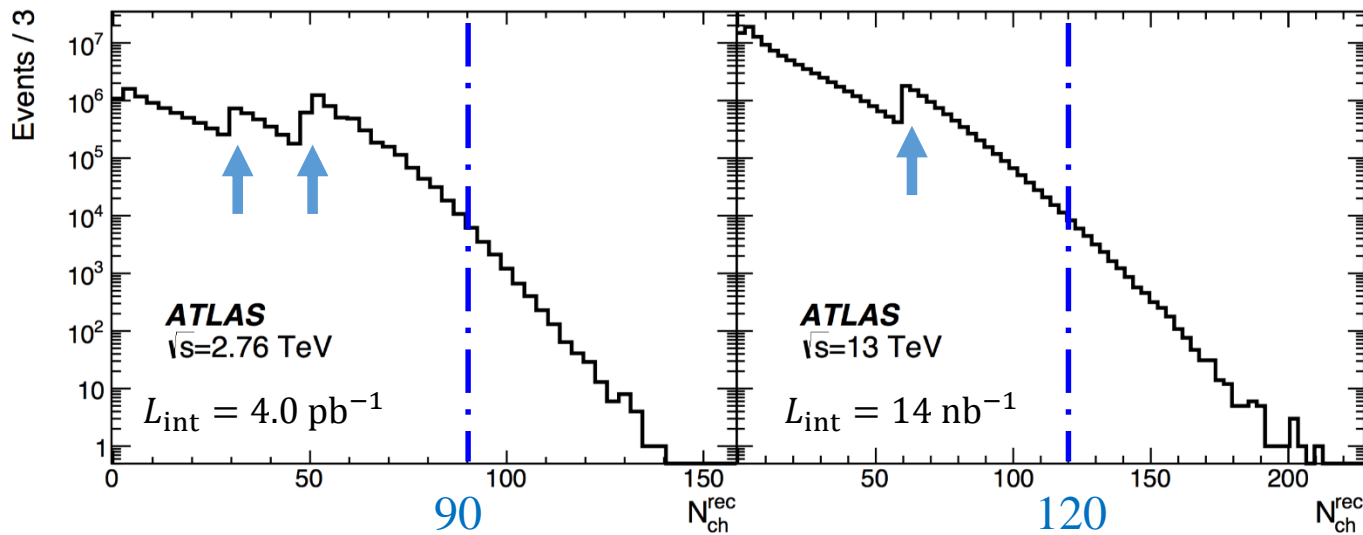
- $|\eta| \leq 2.5$
- $p_T > 0.3$  GeV

$$C(\Delta\eta, \Delta\phi) = \frac{S(\Delta\eta, \Delta\phi)}{B(\Delta\eta, \Delta\phi)}$$



ATLAS Inner Detector

- High-Multiplicity track triggers used to increase statistics.



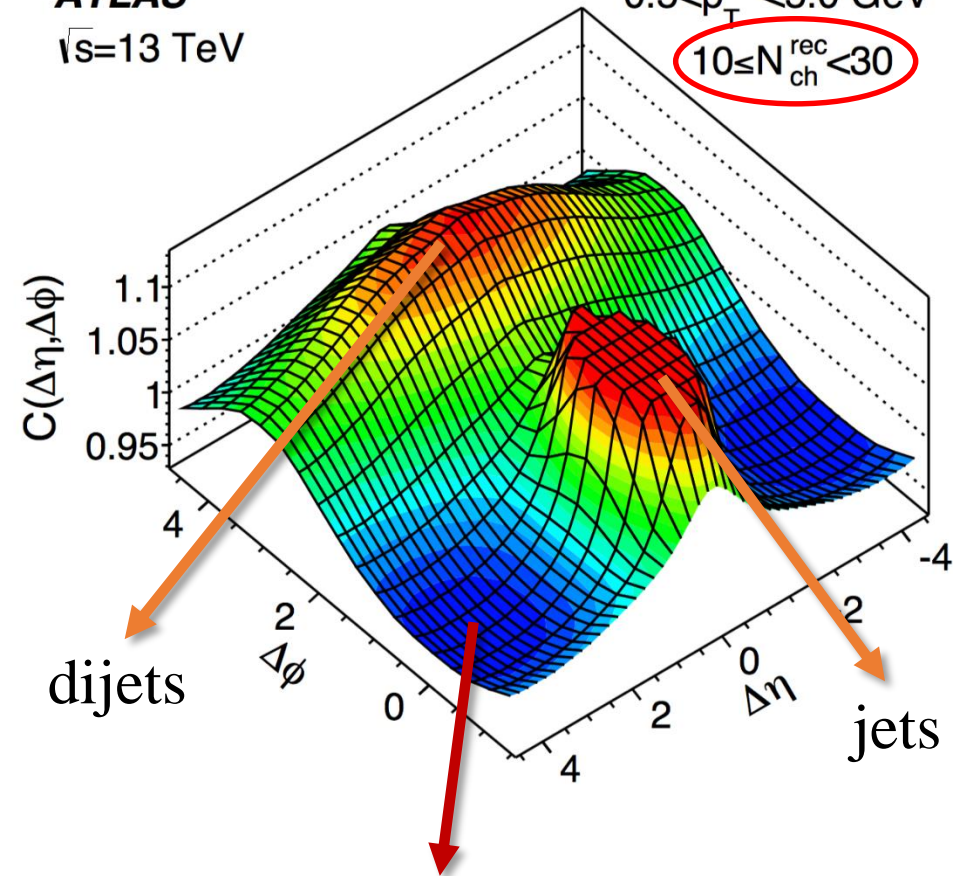
# $C(\Delta\eta, \Delta\phi)$ in 13 TeV $pp$

ATLAS

$\sqrt{s}=13$  TeV

$0.5 < p_T^{a,b} < 5.0$  GeV

$10 \leq N_{ch}^{rec} < 30$

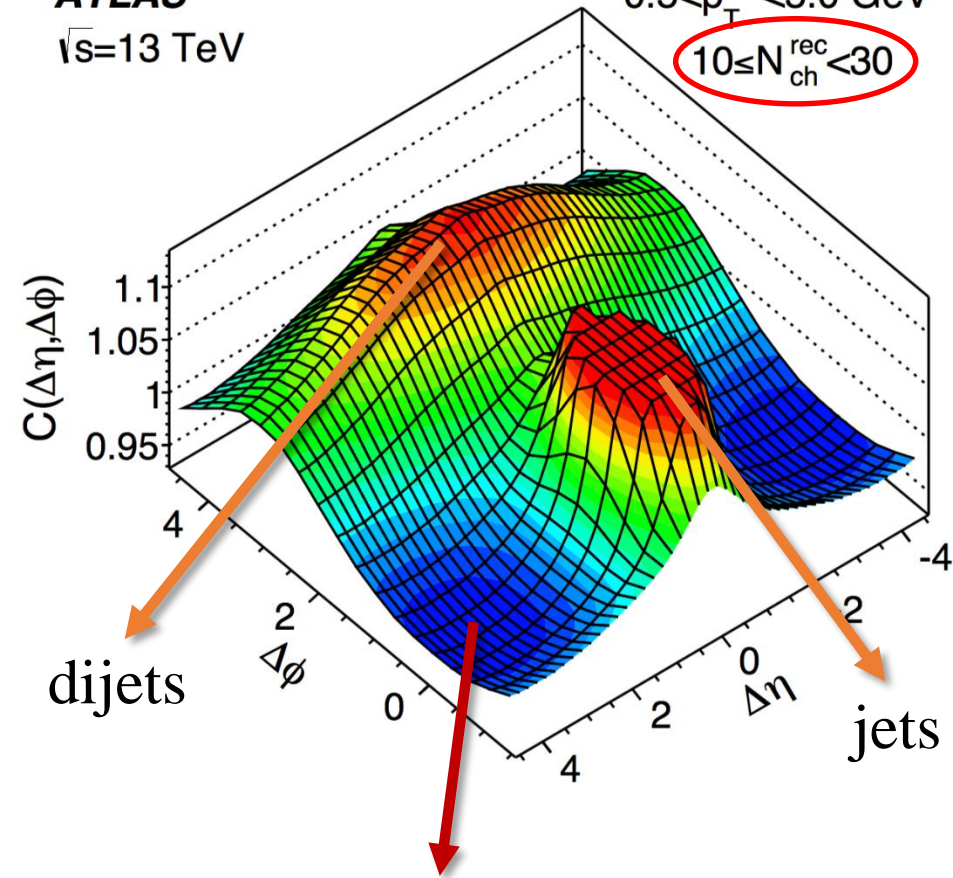


Long-range correlation shape is concave-up on near-side: no ridge.

# $C(\Delta\eta, \Delta\phi)$ in 13 TeV $pp$

**ATLAS**  
 $\sqrt{s}=13$  TeV

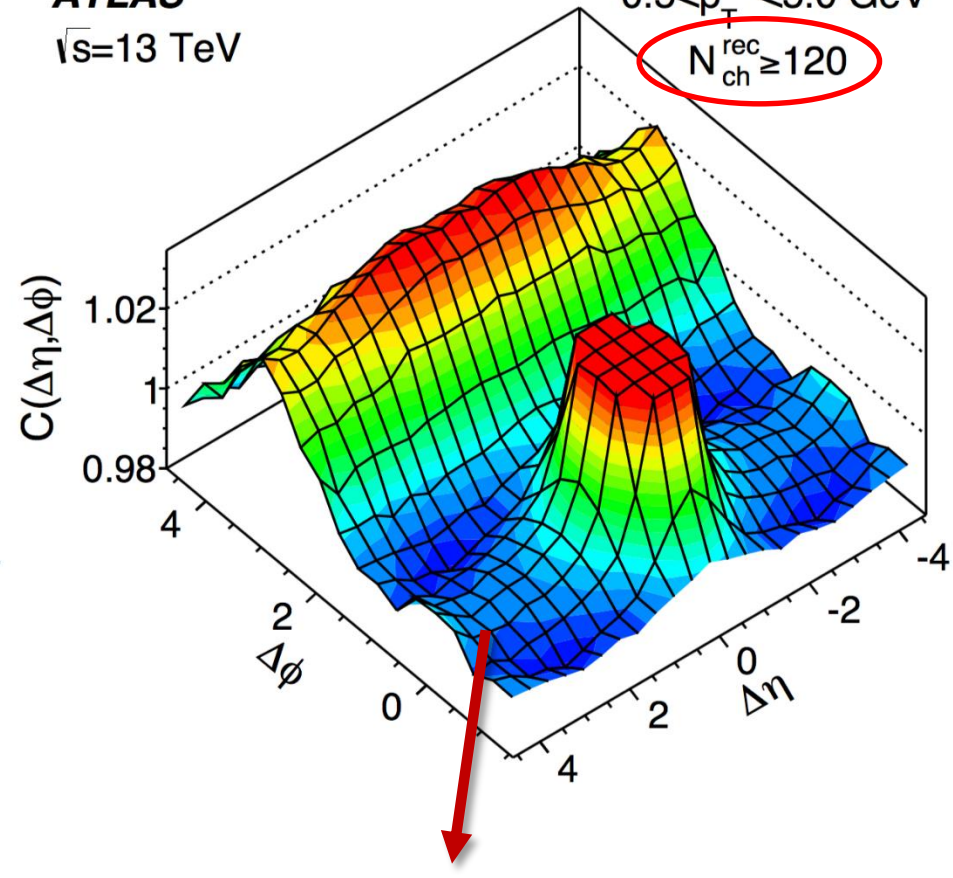
$0.5 < p_T^{a,b} < 5.0$  GeV  
 $10 \leq N_{ch}^{rec} < 30$



Long-range correlation shape is concave-up on near-side: no ridge.

**ATLAS**  
 $\sqrt{s}=13$  TeV

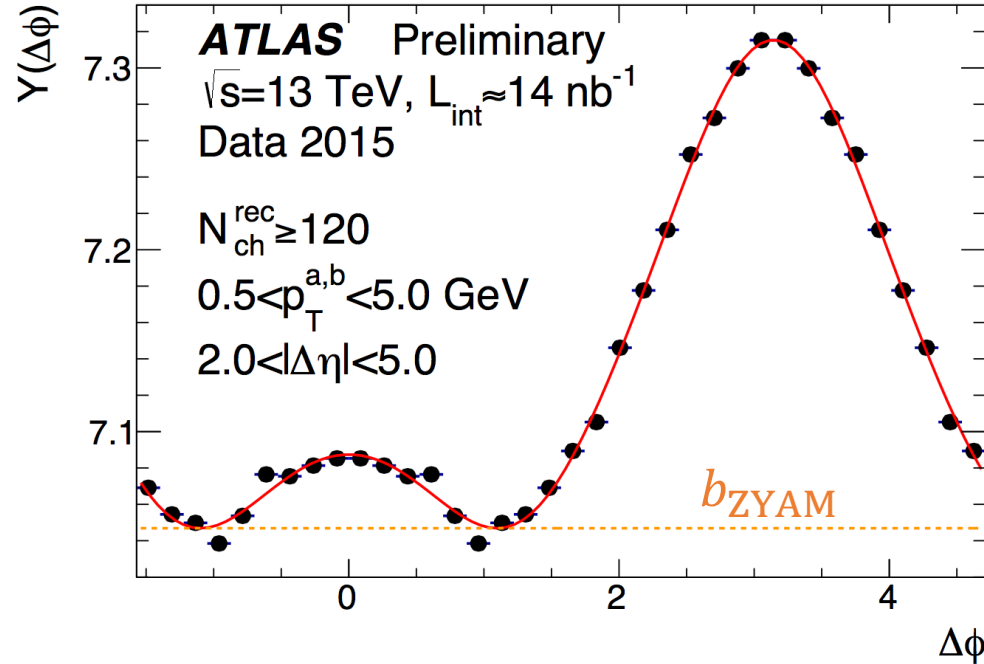
$0.5 < p_T^{a,b} < 5.0$  GeV  
 $N_{ch}^{rec} \geq 120$



Long-range structure becomes flat: ridge develops.



# Ridge yield

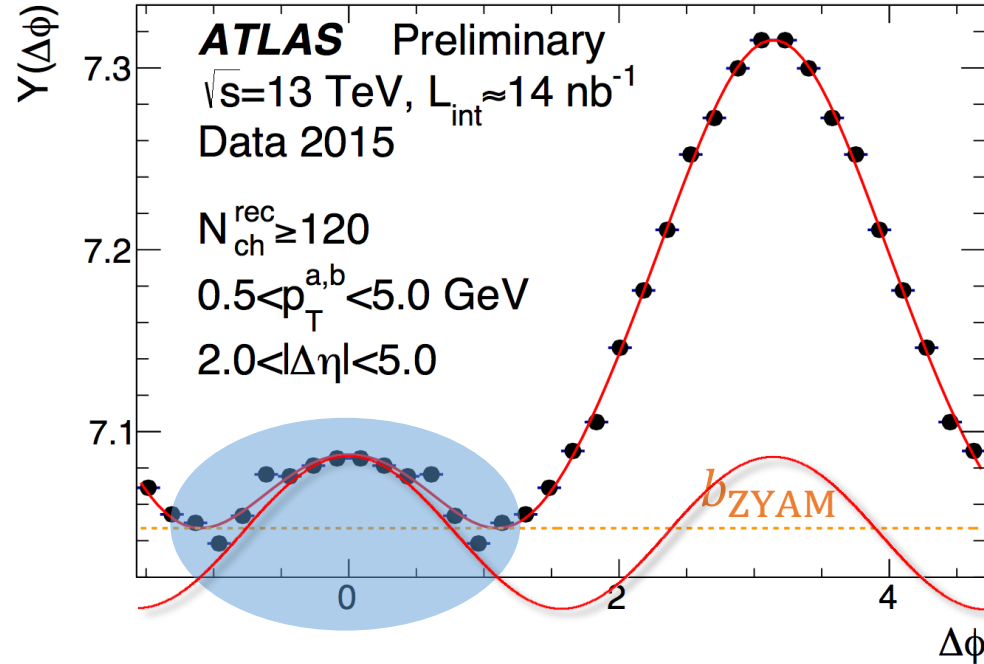


- To quantify the strength of the ridge yield:

$$Y(\Delta\phi) = \left( \frac{\int B(\Delta\phi) d\Delta\phi}{N^a \int d\Delta\phi} \right) C(\Delta\phi)$$

$N^a$  total number of trigger number

# Ridge yield



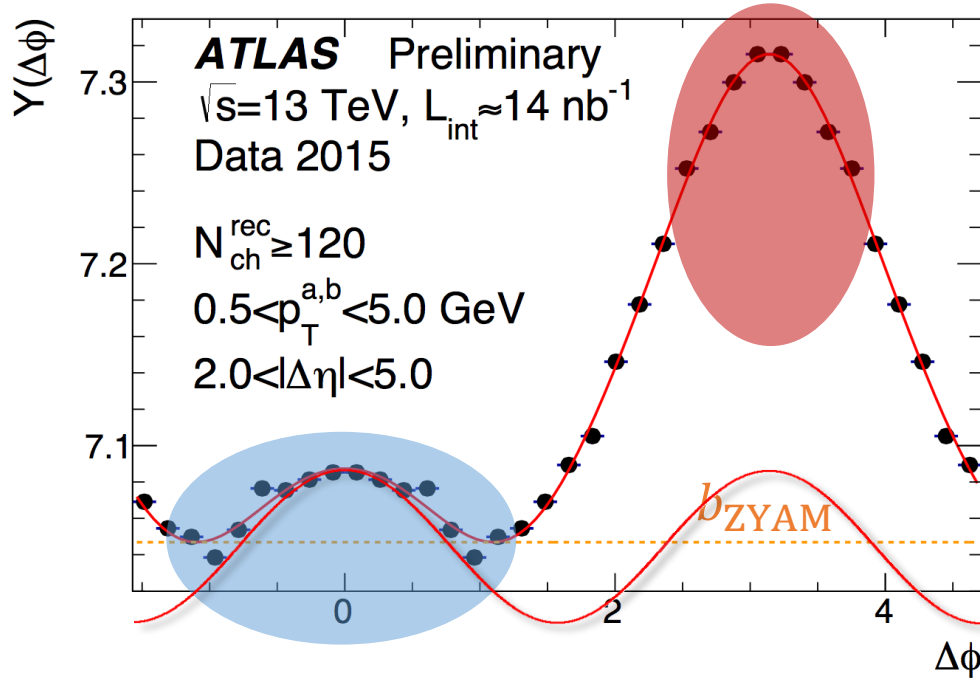
- To quantify the strength of the ridge yield:

$$Y(\Delta\phi) = \left( \frac{\int B(\Delta\phi) d\Delta\phi}{N^a \int d\Delta\phi} \right) C(\Delta\phi)$$

$N^a$  total number of trigger number

- ZYAM method estimates ridge yield in near-side (presented in [EPS 2015](#));
- ZYAM assumes pairs under pedestal  $b_{\text{ZYAM}}$  are uncorrelated;
- Due to the modulation of LRC in near-side, ridge yield may be underestimated.

# Ridge yield



- To quantify the strength of the ridge yield:

$$Y(\Delta\phi) = \left( \frac{\int B(\Delta\phi) d\Delta\phi}{N^a \int d\Delta\phi} \right) C(\Delta\phi)$$

$N^a$  total number of trigger number

- ZYAM method estimates ridge yield in near-side (presented in [EPS 2015](#));
- ZYAM assumes pairs under pedestal  $b_{\text{ZYAM}}$  are uncorrelated;
- Due to the modulation of LRC in near-side, ridge yield may be underestimated.
- Due to dominance of dijet, ZYAM cannot estimate LRC in away-side.
- New method needed!

# Template fitting: two approaches

- Peripheral subtraction  $Y^{\text{LRC}} = Y^{\text{cent}} - F Y^{\text{peri}}$  **Assumption:** shape of away-side jet is independent of  $N_{ch}^{\text{rec}}$ .
- To determine  $F$ :
  - Scale jet yield in near-side;
  - Template fitting (used in this analysis).

**Both ways give consistent results!**

# Template fitting: two approaches

- **Peripheral subtraction**  $Y^{\text{LRC}} = Y^{\text{cent}} - F Y^{\text{peri}}$  **Assumption:** shape of away-side jet is independent of  $N_{ch}^{\text{rec}}$ .
  - **To determine  $F$ :**
    - Scale jet yield in near-side;
    - Template fitting (used in this analysis).
- Both ways give consistent results!**
- **Decompose yield in peripheral**  $Y^{\text{peri}} = N_0^{\text{peri}} + N_0^{\text{peri}} v_{n,n}^{\text{peri}} \cos(n \Delta\phi) + Y_{\text{jet}}^{\text{peri}}$
  - First term represent uncorrelated pairs, second term is LRC in peripheral;
  - **The key is whether including the pedestal  $N_0^{\text{peri}}$  or not!**

# Template fitting: two approaches

- Peripheral subtraction  $Y^{\text{LRC}} = Y^{\text{cent}} - F Y^{\text{peri}}$  **Assumption:** shape of away-side jet is independent of  $N_{ch}^{\text{rec}}$ .
- To determine  $F$ :
  - Scale jet yield in near-side;
  - Template fitting (used in this analysis).

Both ways give consistent results!

- Decompose yield in peripheral  $Y^{\text{peri}} = N_0^{\text{peri}} + N_0^{\text{peri}} v_{n,n}^{\text{peri}} \cos(n \Delta\phi) + Y_{\text{jet}}^{\text{peri}}$
- First term represent uncorrelated pairs, second term is LRC in peripheral;
- The key is whether including the pedestal  $N_0^{\text{peri}}$  or not!

- Expand  $Y^{\text{LRC}}$  and  $Y^{\text{cent}}$ . Denote  $F N_0^{\text{peri}} / N_0^{\text{cent}} \equiv \alpha$ ;

- Exclude pedestal

$$v_{n,n}^{\text{LRC}} = v_{n,n}^{\text{cent}} - \alpha v_{n,n}^{\text{peri}}$$

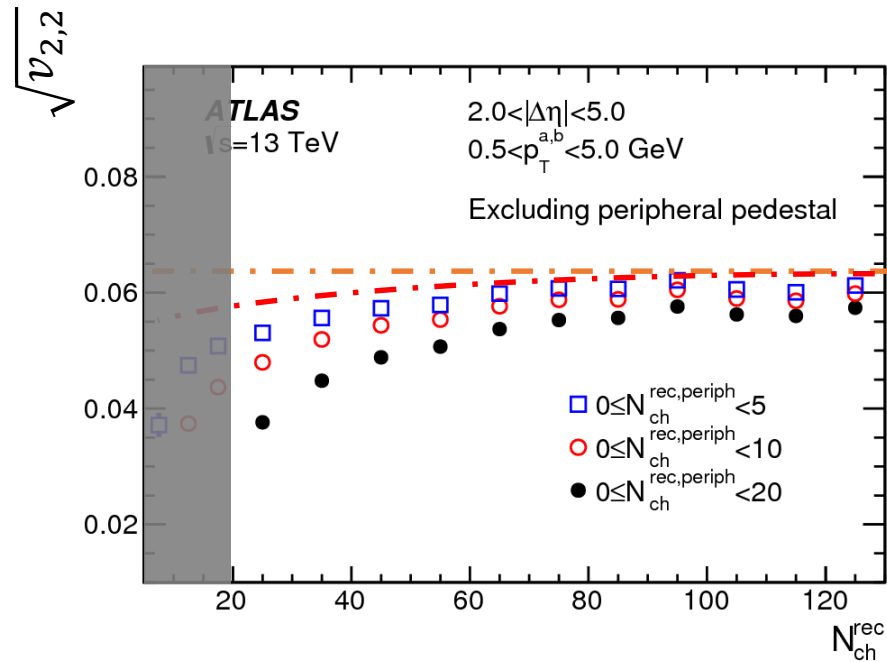
- Include pedestal

$$v_{n,n}^{\text{LRC}} = \frac{v_{n,n}^{\text{cent}} - \alpha v_{n,n}^{\text{peri}}}{1 - \alpha}$$

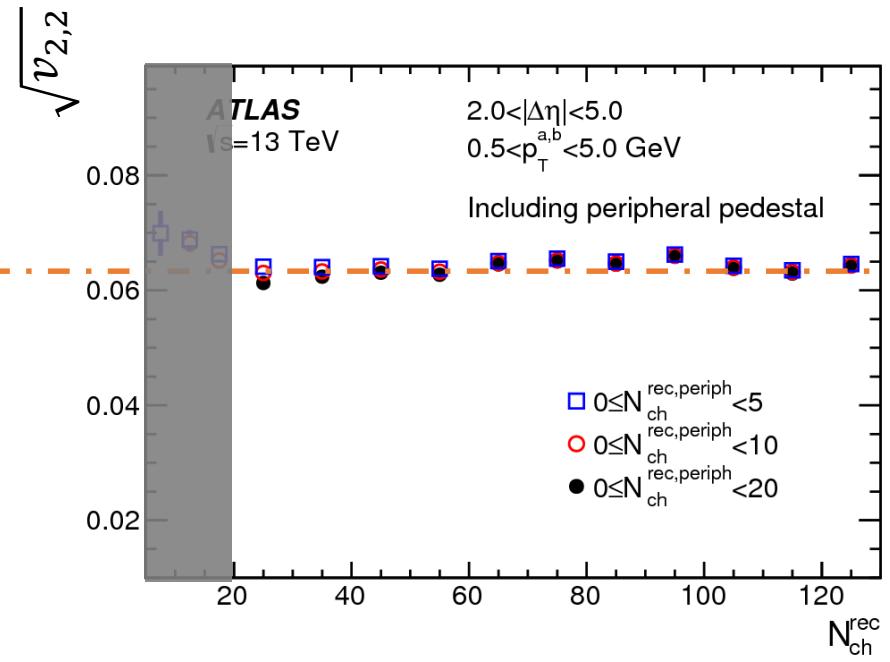
Only differentiate by a scale factor  $1 - \alpha$  !

# Comparison of two template fit methods

Exclude Pedestal



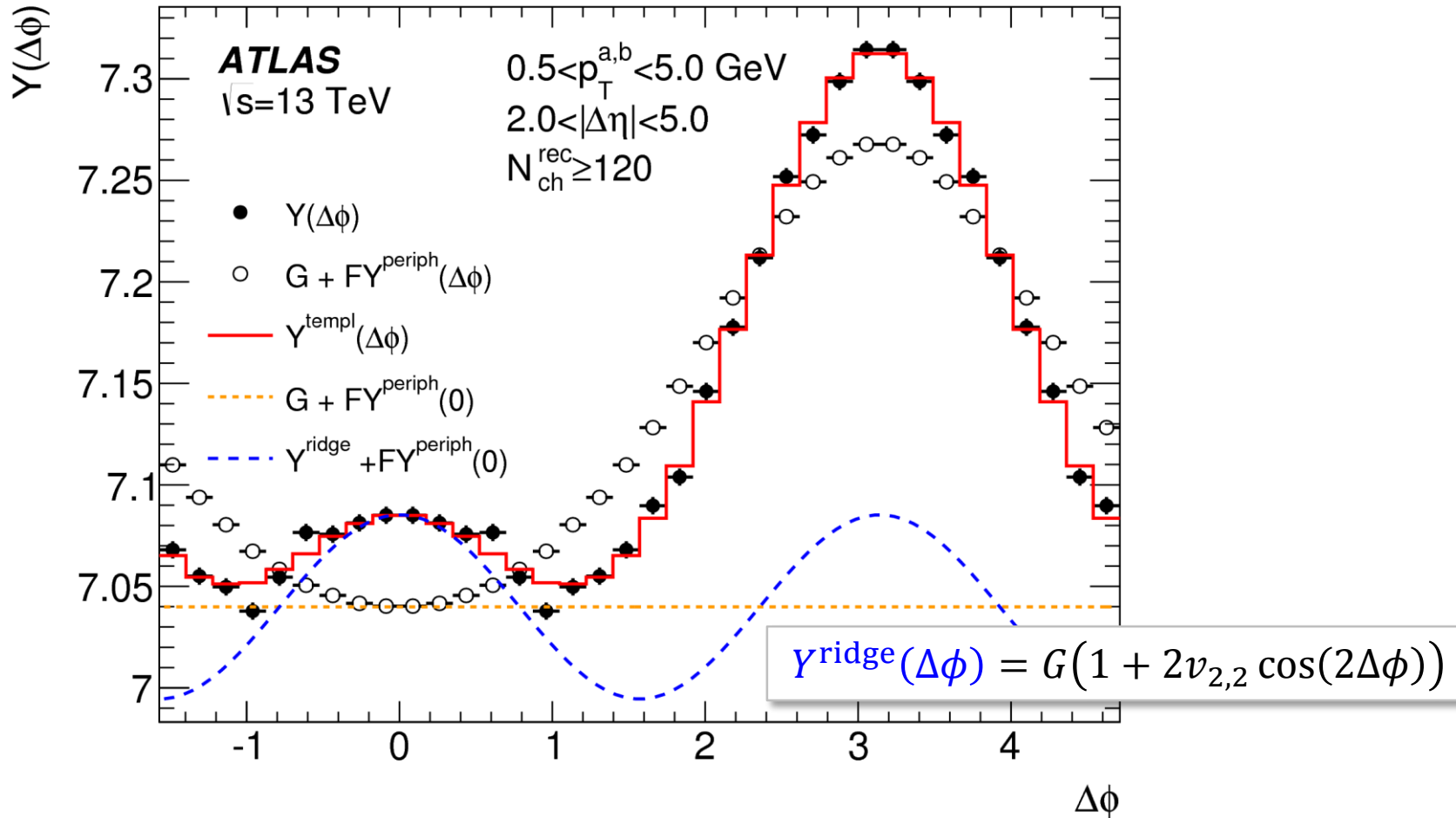
Include Pedestal



- Two methods represents two limits, however, **they give similar LRC signal for  $N_{ch}^{rec} \geq 20$** . The true value of  $v_{2,2}$  lies between two bounds.
- In this analysis, default results are from including pedestal, for  $N_{ch}^{rec} \geq 20$ .

# Template fitting results

$$Y^{\text{templ}}(\Delta\phi) = Y^{\text{ridge}}(\Delta\phi) + FY^{\text{periph}}(\Delta\phi)$$

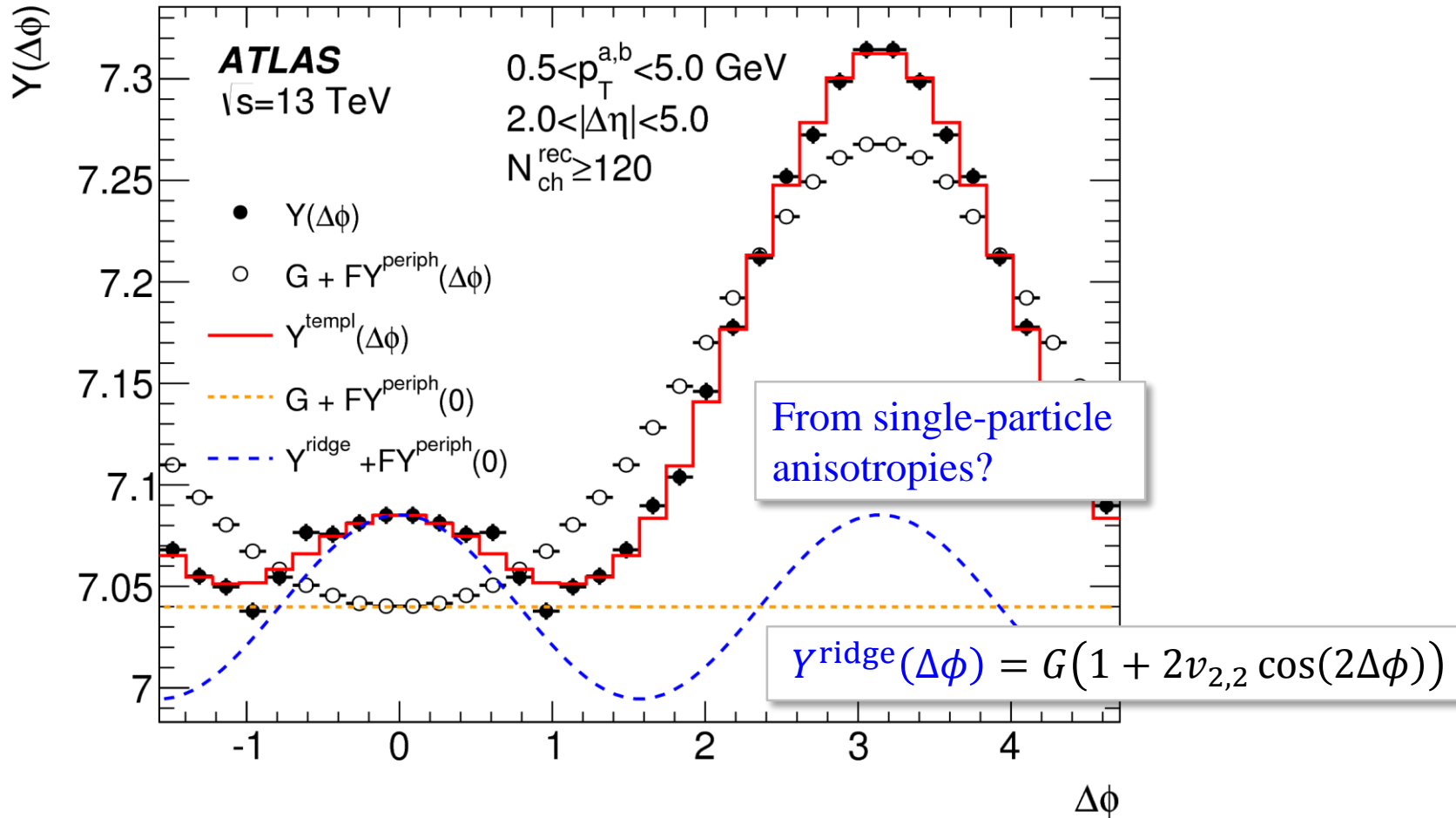


- Template fitting works quite well: compare red curve  $Y^{\text{templ}}$  and black bullets  $Y$ .



# Template fitting results

$$Y^{\text{templ}}(\Delta\phi) = Y^{\text{ridge}}(\Delta\phi) + FY^{\text{periph}}(\Delta\phi)$$



- Template fitting works quite well: compare red curve  $Y^{\text{templ}}$  and black bullets  $Y$ .

# Single-particle anisotropies $v_2$

- In Pb+Pb and  $p$ +Pb collisions, the long-range structures in two-particle correlation arise from single particle anisotropies

$$\text{Singles: } \frac{dN}{d\phi} \propto 1 + \sum_n 2v_n \cos n(\phi - \Phi_n)$$

$$\Rightarrow \text{Pairs: } \frac{dN}{d\Delta\phi} \propto 1 + \sum_n 2v_n^a v_n^b \cos n(\Delta\phi)$$

- If this is also true in  $pp$ , then the measured  $v_{2,2}$  should factorize as:

$$v_{2,2}(p_T^a, p_T^b) = v_2(p_T^a) v_2(p_T^b)$$

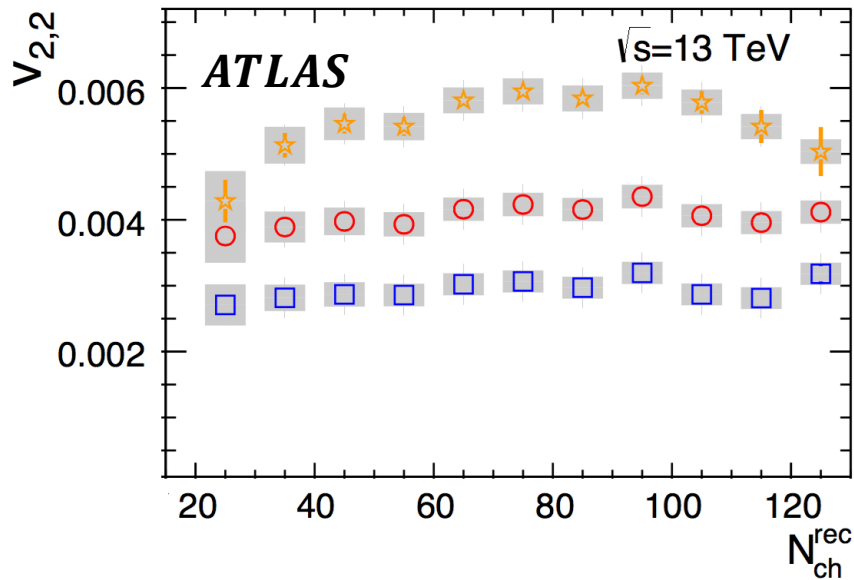
$$\Rightarrow v_2(p_T^a) = v_{2,2}(p_T^a, p_T^b) / \sqrt{v_{2,2}(p_T^b, p_T^b)}$$

- **Expectation:**  $v_{2,2}(p_T^a, p_T^b)$  depends on both  $p_T^a$  and  $p_T^b$ , but the ratio  $v_2(p_T^a)$  should be independent of reference  $p_T^b$ .

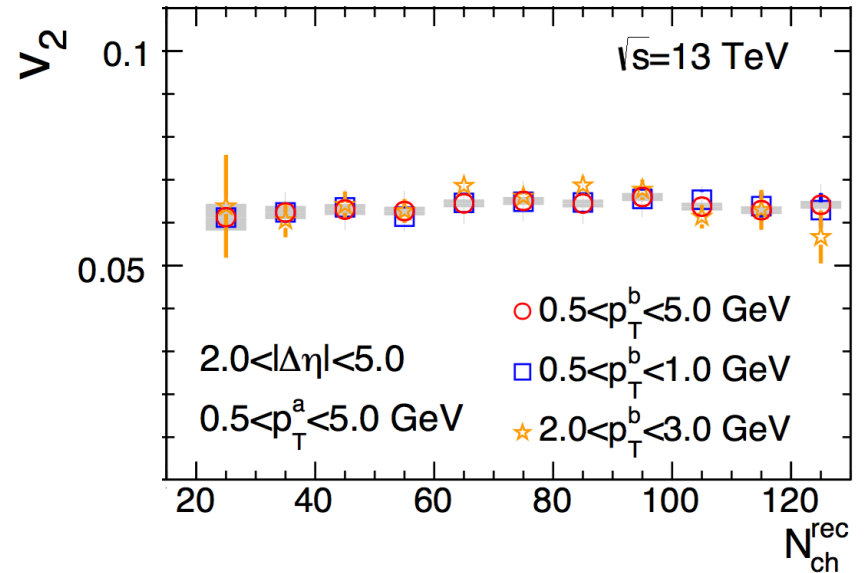
# Factorization of $v_{2,2}$

- **Expectation:**  $v_{2,2}(p_T^a, p_T^b)$  depends on both  $p_T^a$  and  $p_T^b$ , but the ratio  $v_2(p_T^a)$  should be independent of reference  $p_T^b$ .

# Factorization of $v_{2,2}$



- $v_{2,2}$  is dependent of  $p_T^b$ .

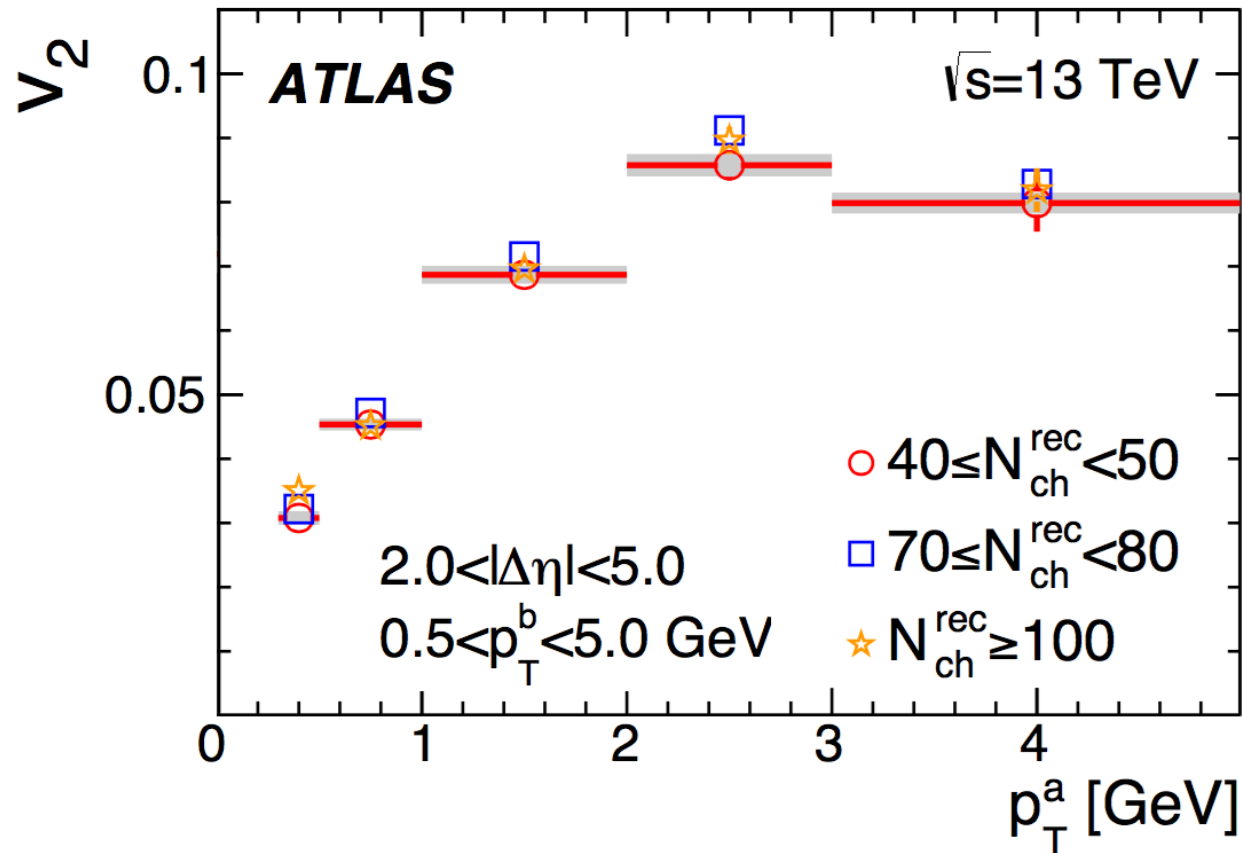


- $v_2$  is independent of  $p_T^b$ .

$v_{2,2}$  can be factorized into single-particle  $v_2$ .

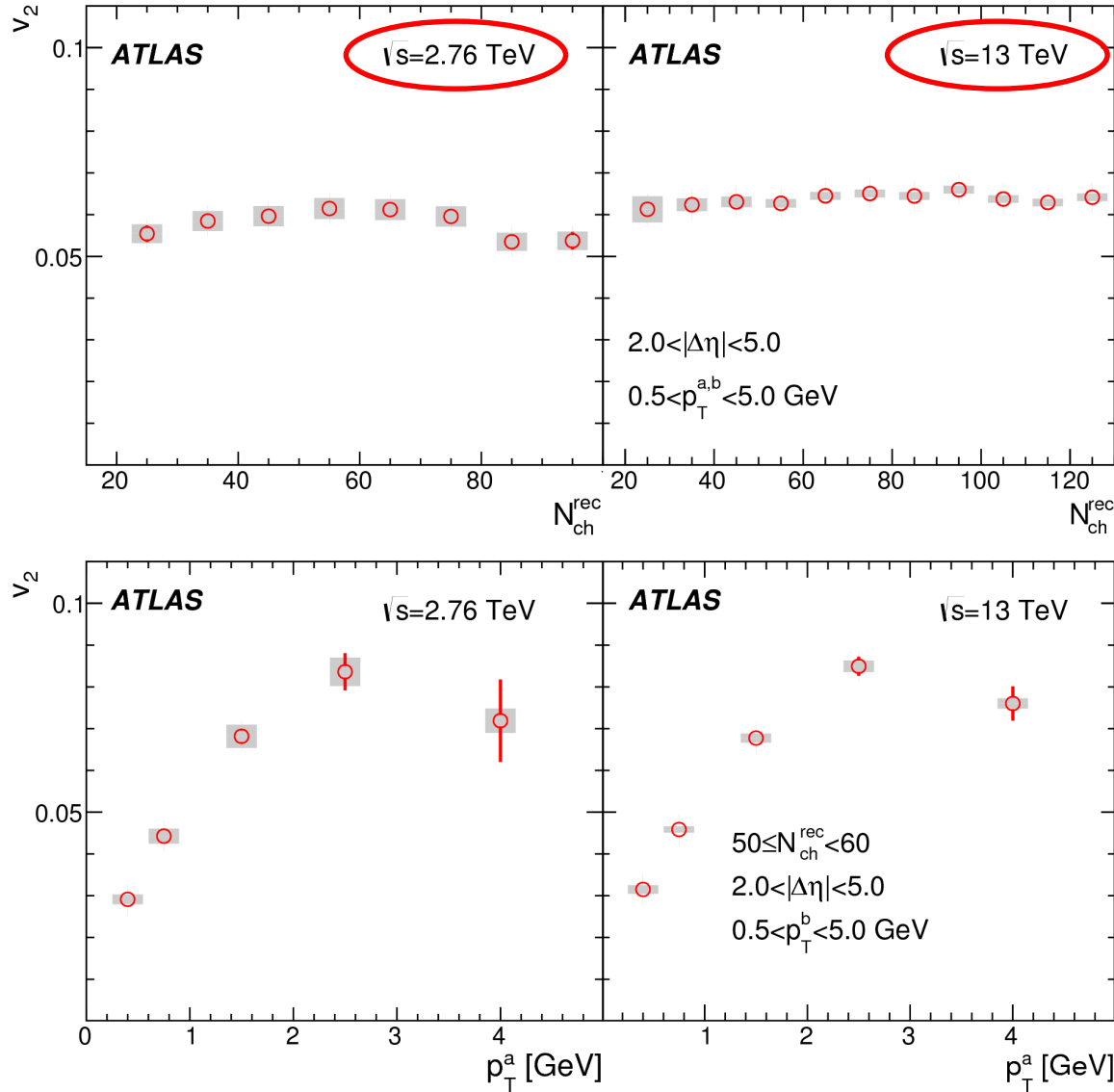
- **Expectation:**  $v_{2,2}(p_T^a, p_T^b)$  depends on both  $p_T^a$  and  $p_T^b$ , but the ratio  $v_2(p_T^a)$  should be independent of reference  $p_T^b$ .

# $p_T$ dependence of $v_2$



- $v_2$  increases with  $p_T$  at lower  $p_T$ ;
- Reaches a maximum between 2 and 3 GeV;
- Decreases at higher  $p_T$ .

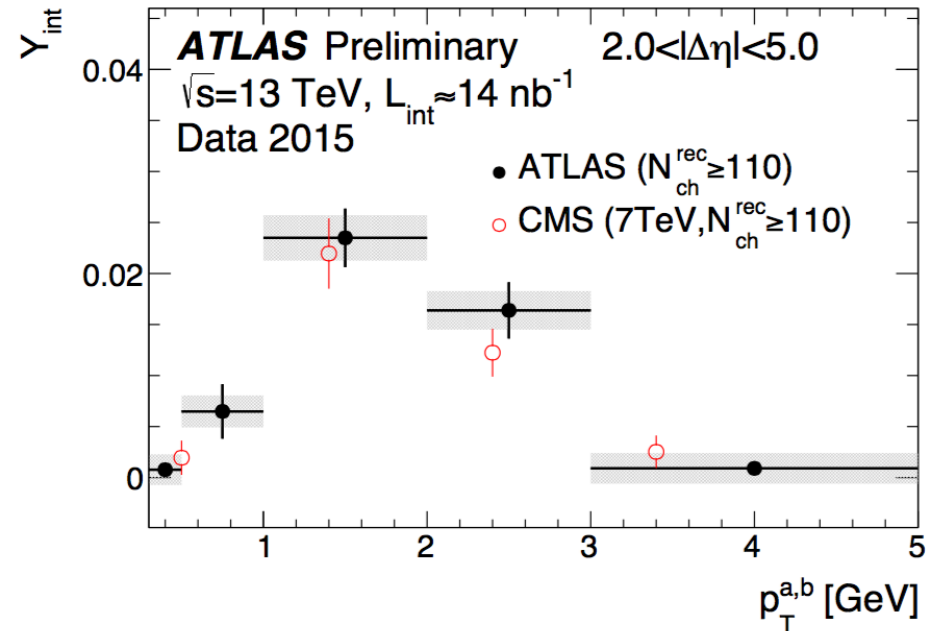
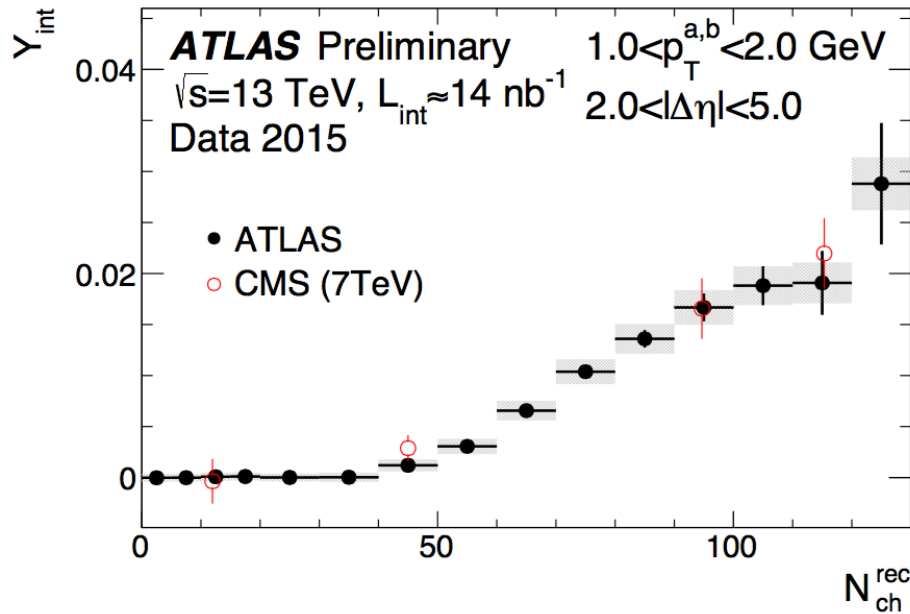
# Energy dependence of $v_2$



$v_2$  has a very weak energy dependence.

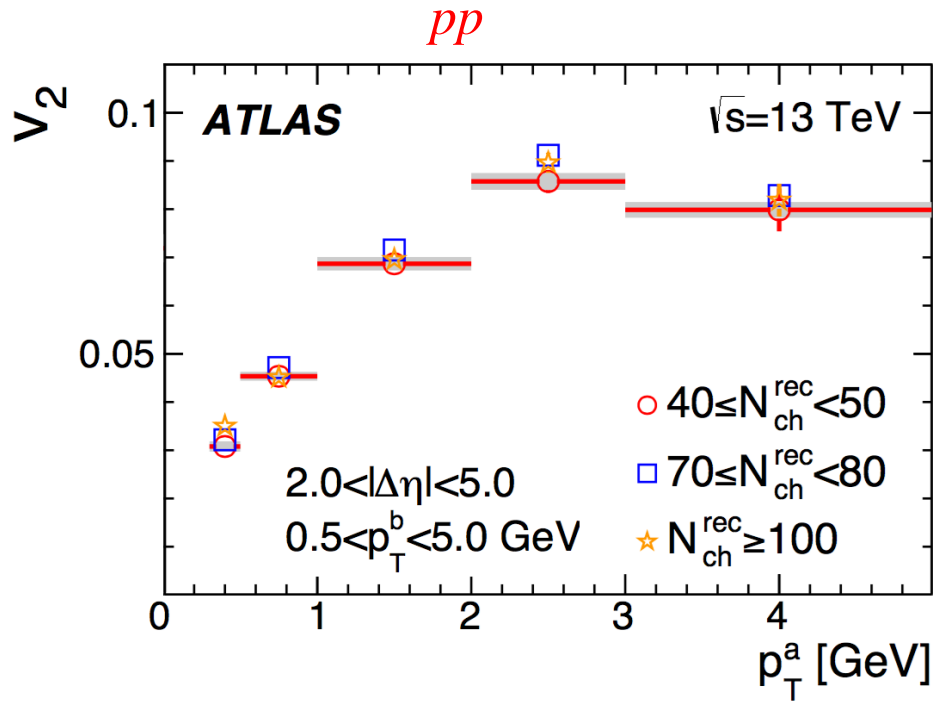
# Energy dependence of integrated yield

$$Y_{\text{int}} = \int_{-\Delta\phi_{ZYAM}}^{\Delta\phi_{ZYAM}} d\Delta\phi (Y(\Delta\phi) - b_{ZYAM})$$

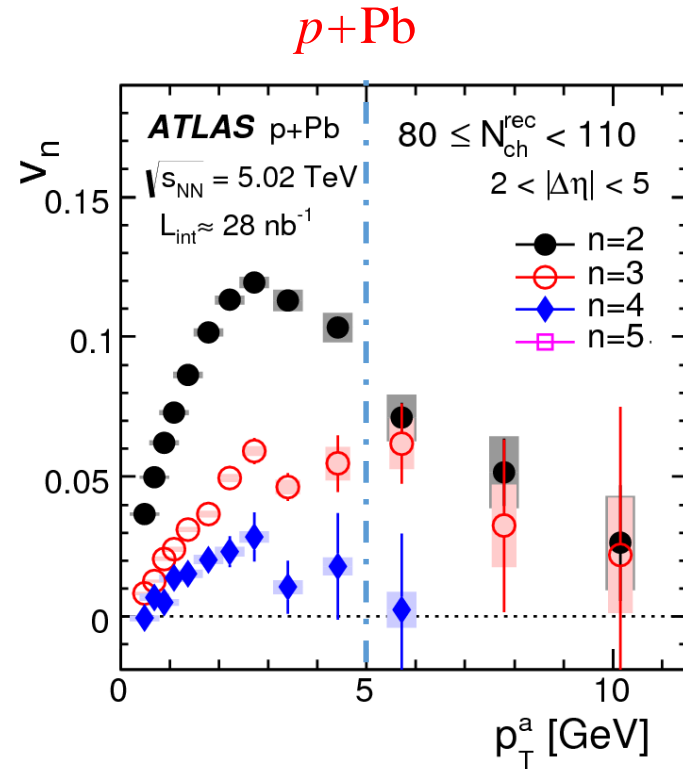


Integrated yield has a very weak energy dependence.

# Different collision systems



- $v_2$  have similar trend, but 30% smaller in *pp*;
- Suggesting a similar physical mechanism?





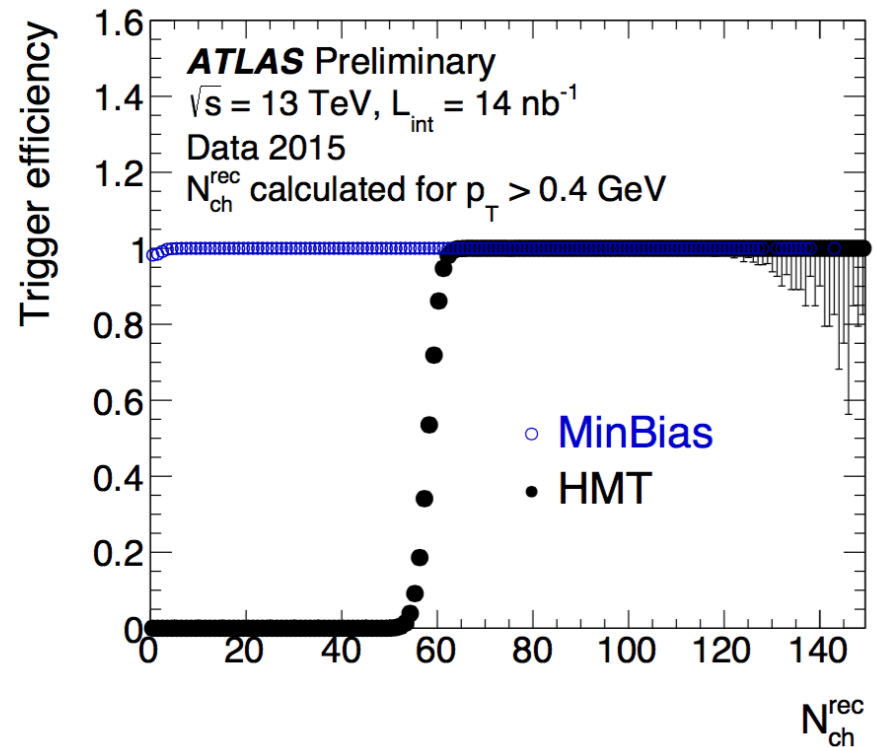
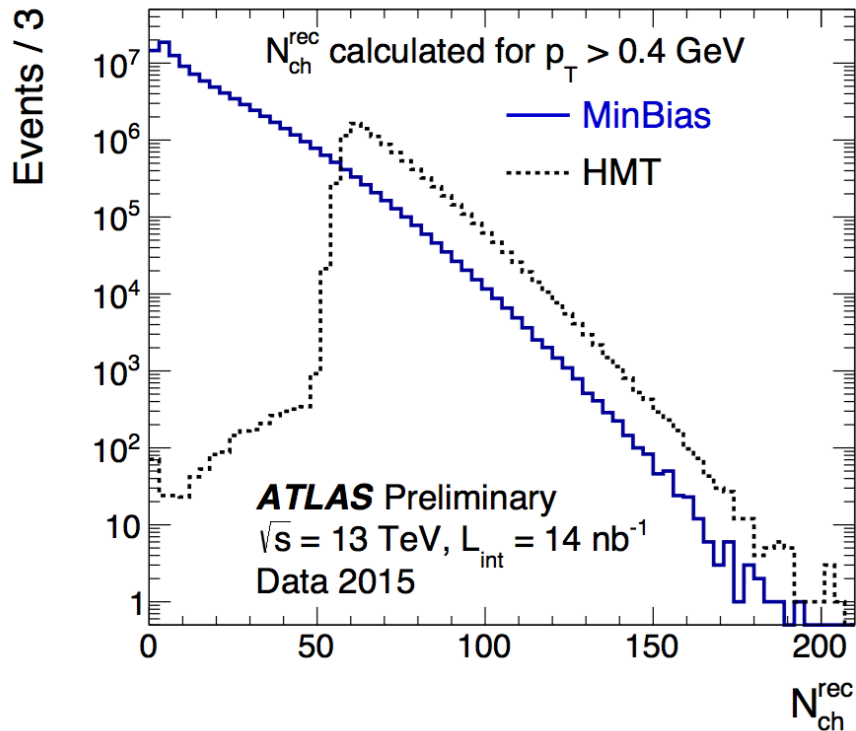
# Summary

- Ridge observed in high-multiplicity  $pp$  collisions at 13 and 2.76 TeV;
- Template fitting is applied to extract LRC modulated by  $v_{2,2}$ ;
- $v_{2,2}$  can be factorized into single particle  $v_2$ ;
- $v_2$  has a very weak  $N_{ch}^{rec}$  dependence;
- $v_2$  has a very weak energy dependence;
- $v_2$  has a similar trend as  $p+Pb$ .

# Back-up

# More about the data set

- 13 TeV data were collected in low-luminosity runs for which the collision rate per crossing,  $\mu$ , varied between  $\sim 0.002$  and  $\sim 0.04$ ;
- **The major high-multiplicity track trigger**
  - At least one counter on each side of the MBTS;
  - At least 900 hits in the SCT;
  - At least 60 HLT-reconstructed tracks having  $p_T > 0.4$  GeV.



# Systematics for $v_{2,2}$ at $\sqrt{s} = 13$ TeV

	Syst Uncertainty	Value for $v_{2,2}$	Comment
1	Choice of peripheral bin	10% : $N_{ch}^{rec} < 30$ 5-2% : $30 < N_{ch}^{rec} < 60$ 2% : $N_{ch}^{rec} > 60$	$N_{ch}^{rec}$ dependent
2	Tracking Efficiency	0.5%	
3	Pileup	0.25%	
4	MC Closure	2% for $p_T > 0.5$ GeV 6% for $p_T < 0.5$ GeV $1.5 \times 10^{-4}$ (absolute)	Larger of the three numbers for each $p_T^a$
5	Pair Acceptance	$4 \times 10^{-5}$	Absolute error (not %)

- **Choice of Peripheral Bin:** vary the peripheral reference bins  $N_{ch}^{rec}$ ;
- **Tracking Efficiency:** repeat the analysis when varying the efficiency to its upper and lower extremes;
- **Pileup:** fraction of events with pileup vertex close to the primary vertex;
- **MC Consistency:**  $v_{2,2}$  introduced by away-side jet in PYTHIA (no genuine long-range correlation);
- **Pair Acceptance:**  $v_{2,2}$  calculated from the mixed events.

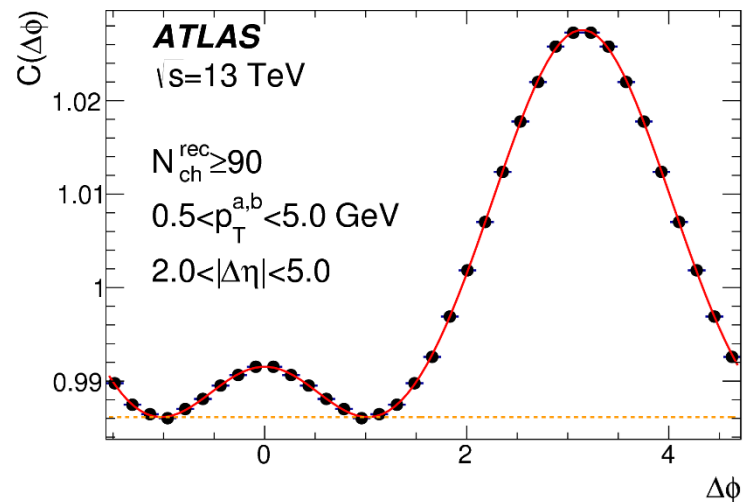
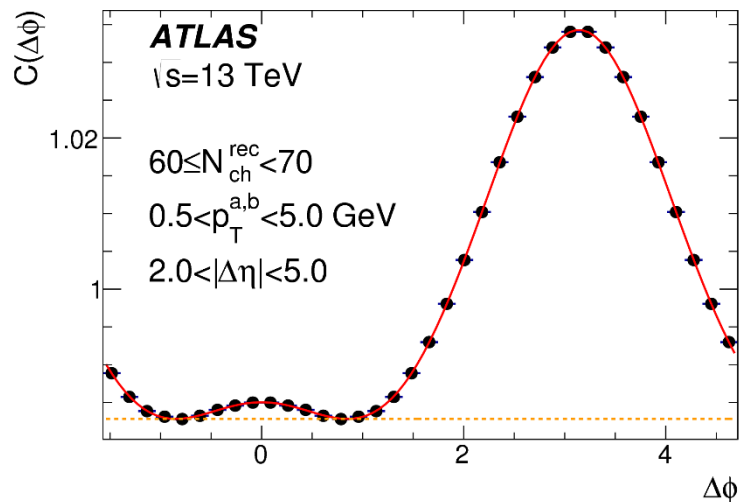
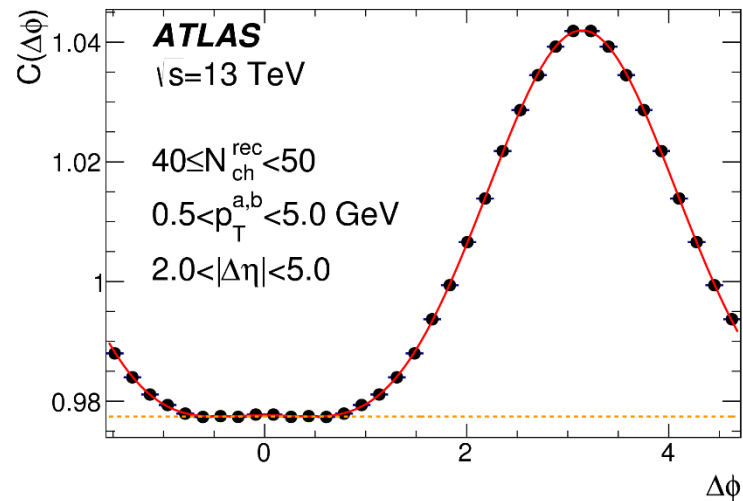
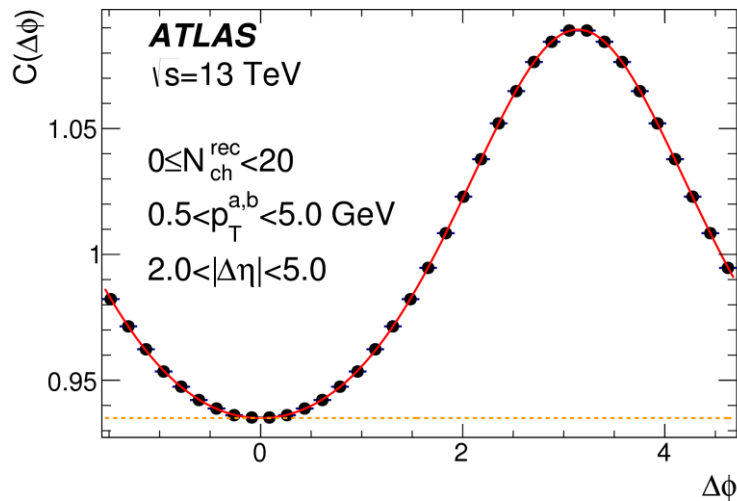
# Systematics for $v_{2,2}$ at $\sqrt{s} = 2.76$ TeV

	Syst Uncertainty	Value for $v_{2,2}$
1	Tracking Efficiency	0.8%
2	MC Closure	2%
3	Pair Acceptance	1%
4	Choice of peripheral bin	6%
5	Pileup	5%

- **Choice of Peripheral Bin:** vary the peripheral reference bins  $N_{ch}^{rec}$ ;
- **Tracking Efficiency:** repeat the analysis when varying the efficiency to its upper and lower extremes;
- **Pileup:** fraction of events with pileup vertex close to the primary vertex;
- **MC Consistency:**  $v_{2,2}$  introduced by away-side jet in PYTHIA (no genuine long-range correlation);
- **Pair Acceptance:**  $v_{2,2}$  calculated from the mixed events.

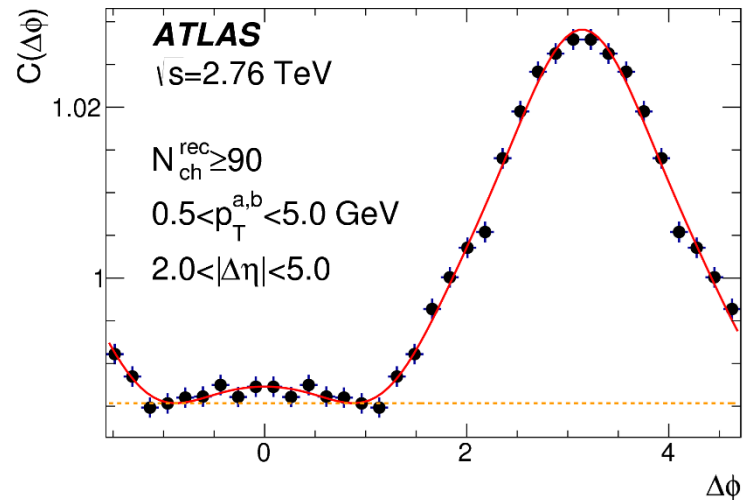
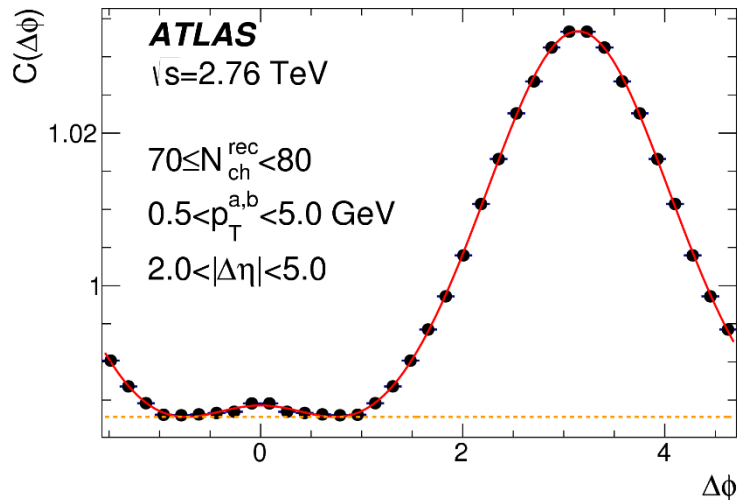
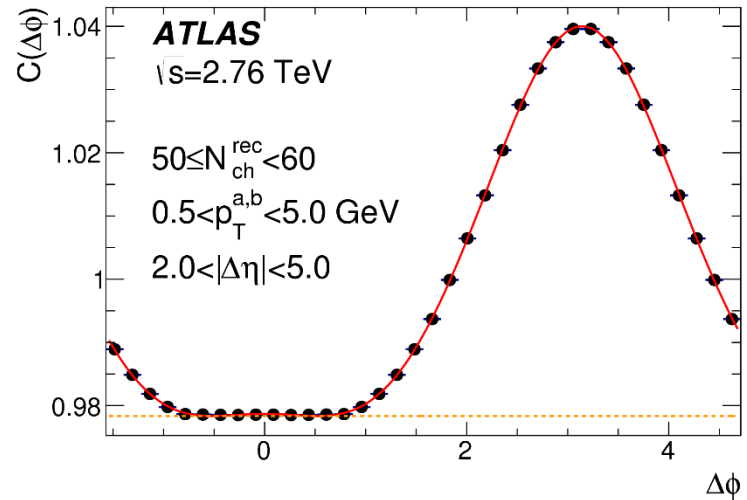
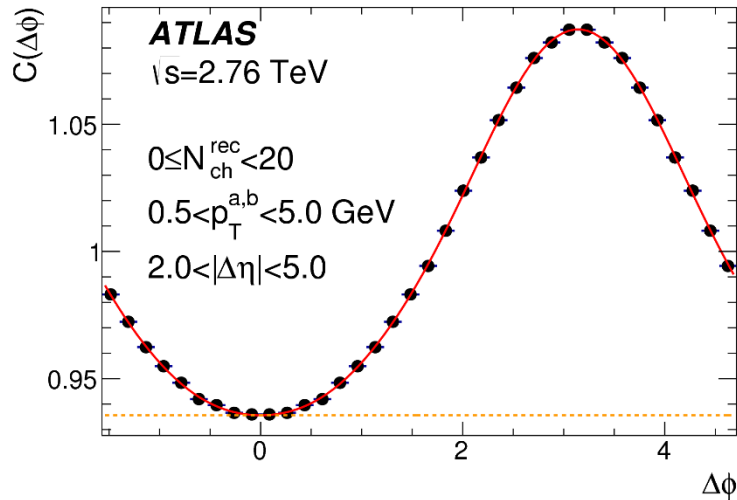
# 1D Correlation functions $C(\Delta\phi)$ at 13 TeV

$$C(\Delta\phi) = \frac{\int_2^5 d|\Delta\phi| S(\Delta\phi, |\Delta\eta|)}{\int_2^5 d|\Delta\phi| B(\Delta\phi, |\Delta\eta|)}$$



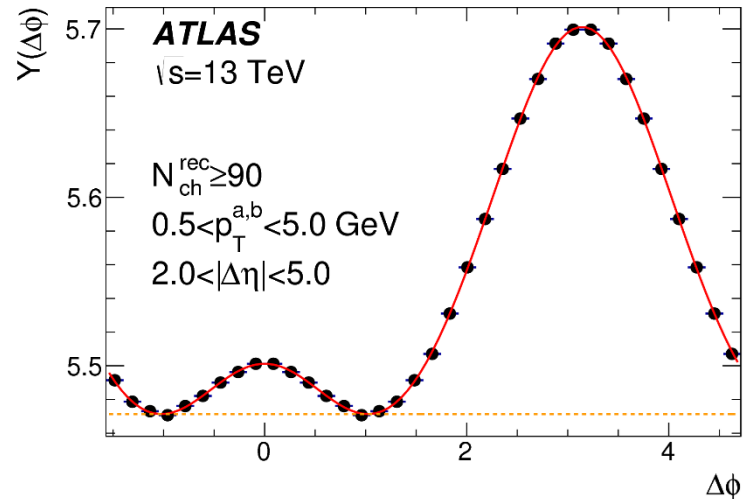
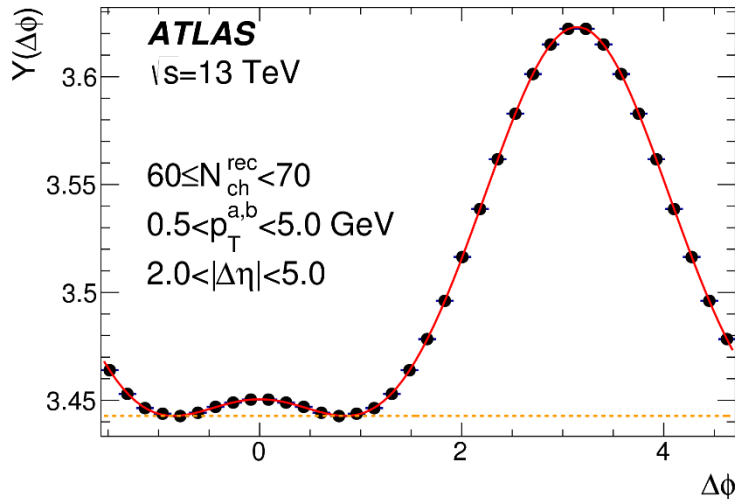
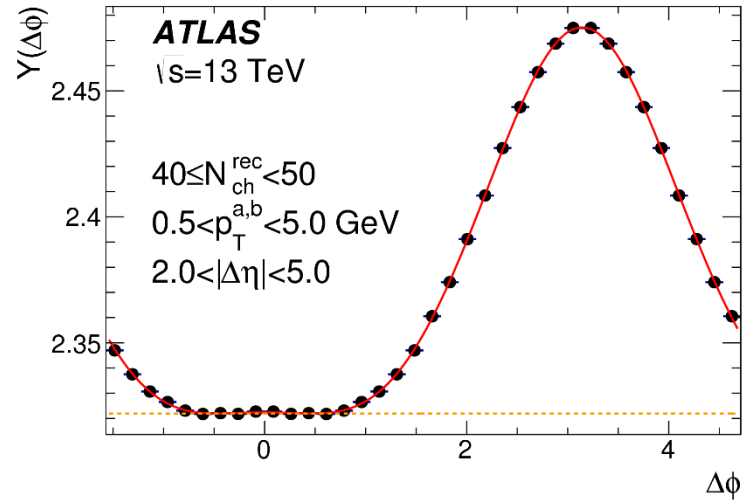
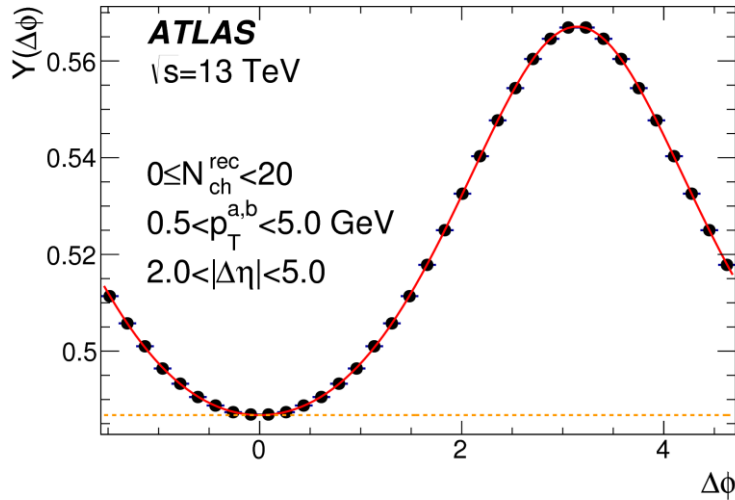
# 1D Correlation functions $C(\Delta\phi)$ at 2.76 TeV

$$C(\Delta\phi) = \frac{\int_2^5 d|\Delta\phi| S(\Delta\phi, |\Delta\eta|)}{\int_2^5 d|\Delta\phi| B(\Delta\phi, |\Delta\eta|)}$$



# Per-trigger-particle yield $Y(\Delta\phi)$ at 13 TeV

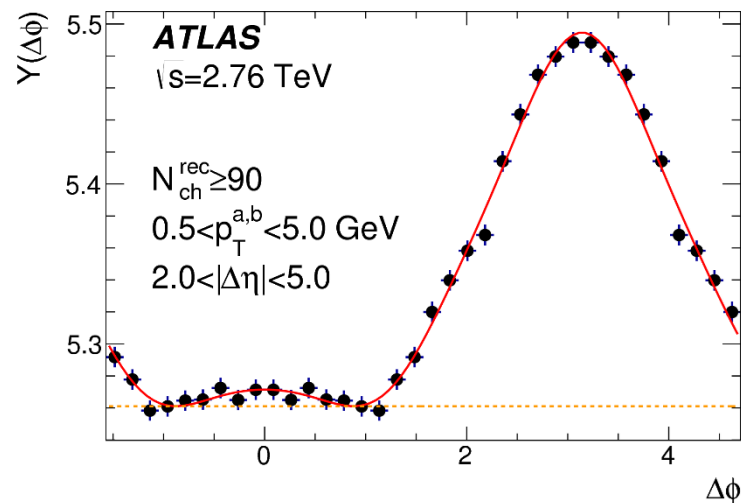
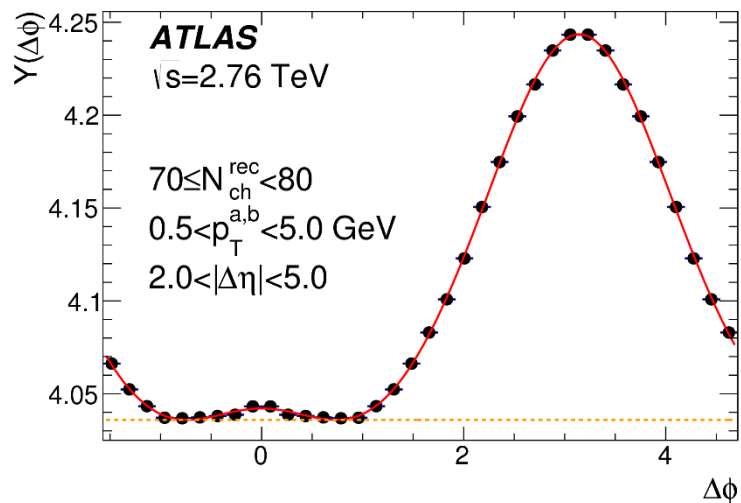
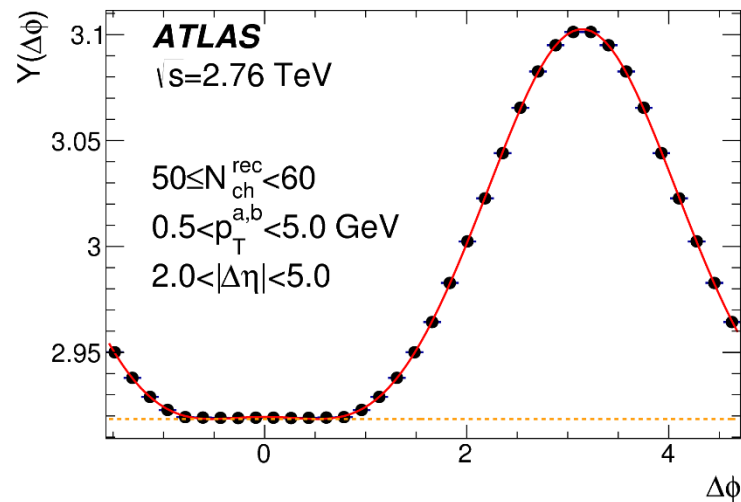
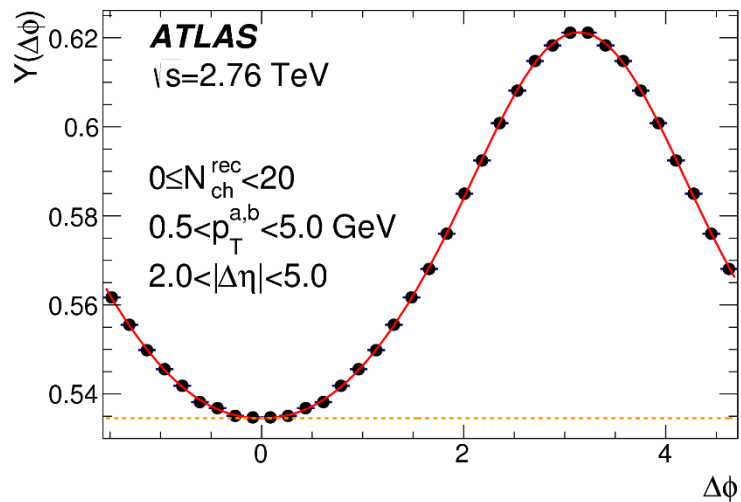
$$Y(\Delta\phi) = \left( \frac{\int B(\Delta\phi) d\Delta\phi}{N^a \int d\Delta\phi} \right) C(\Delta\phi)$$





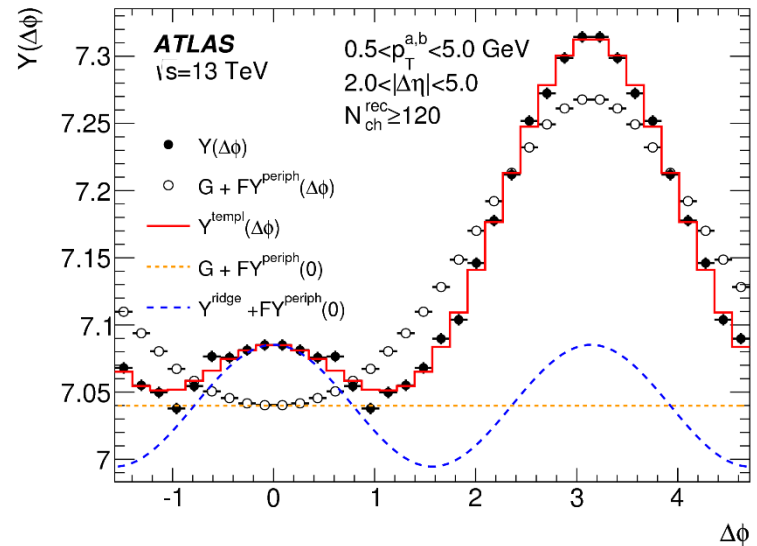
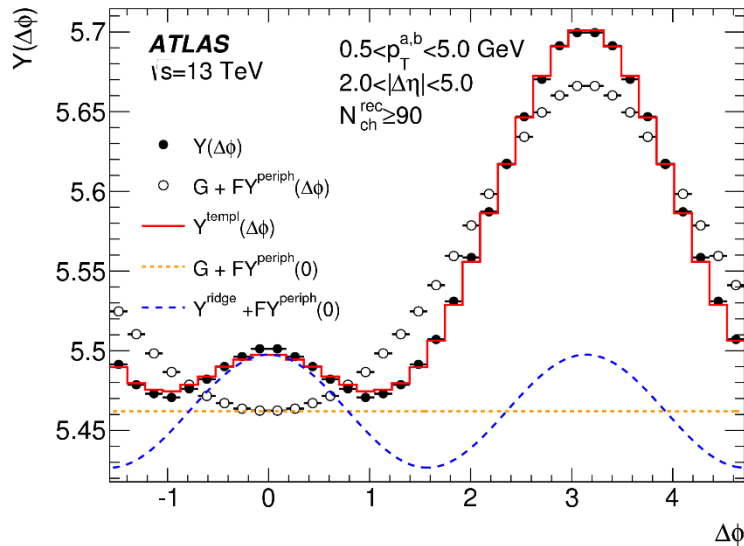
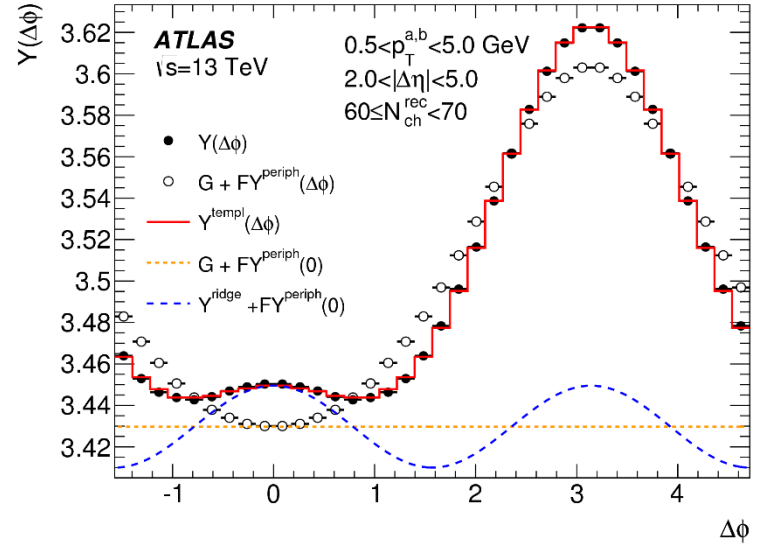
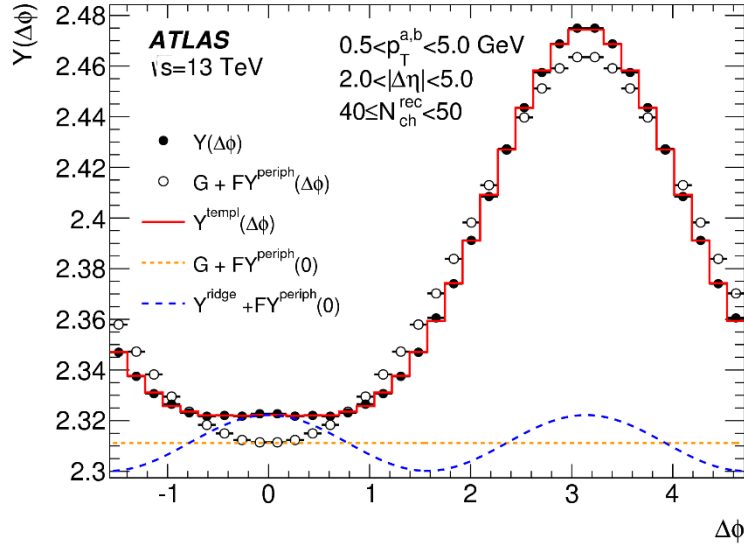
# Per-trigger-particle yield $Y(\Delta\phi)$ at 2.76 TeV

$$Y(\Delta\phi) = \left( \frac{\int B(\Delta\phi) d\Delta\phi}{N^a \int d\Delta\phi} \right) C(\Delta\phi)$$



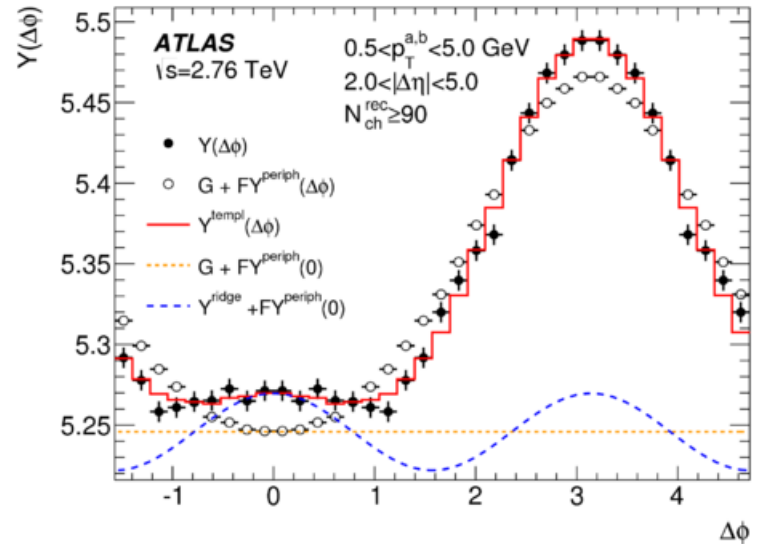
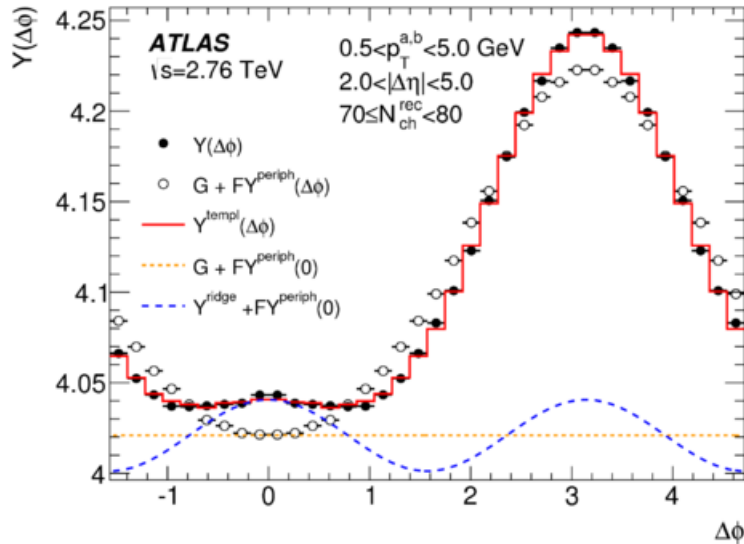
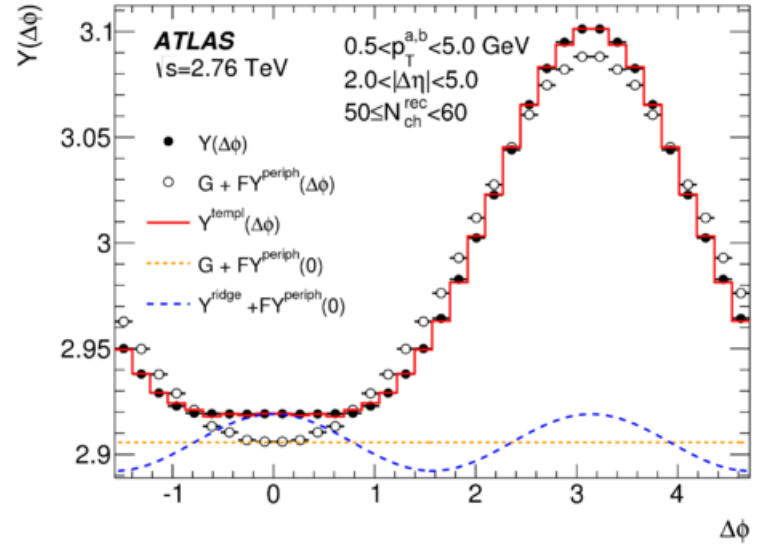
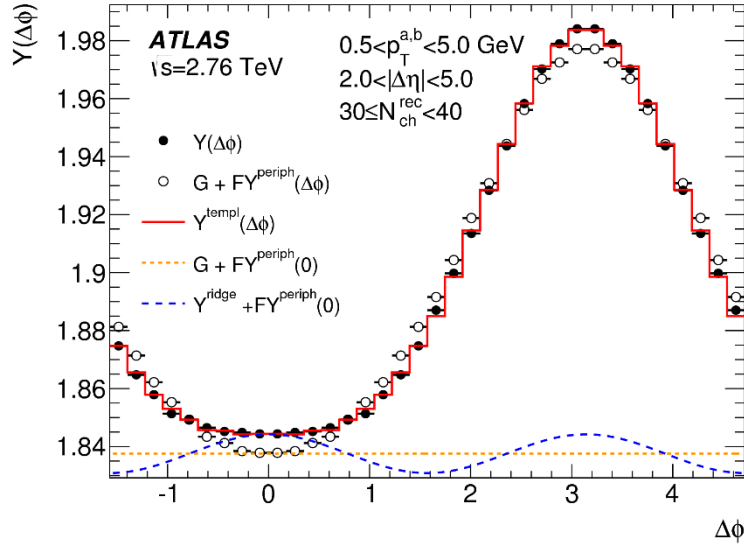
# Template fit at 13 TeV

$$Y^{\text{templ}}(\Delta\phi) = Y^{\text{ridge}}(\Delta\phi) + FY^{\text{periph}}(\Delta\phi)$$

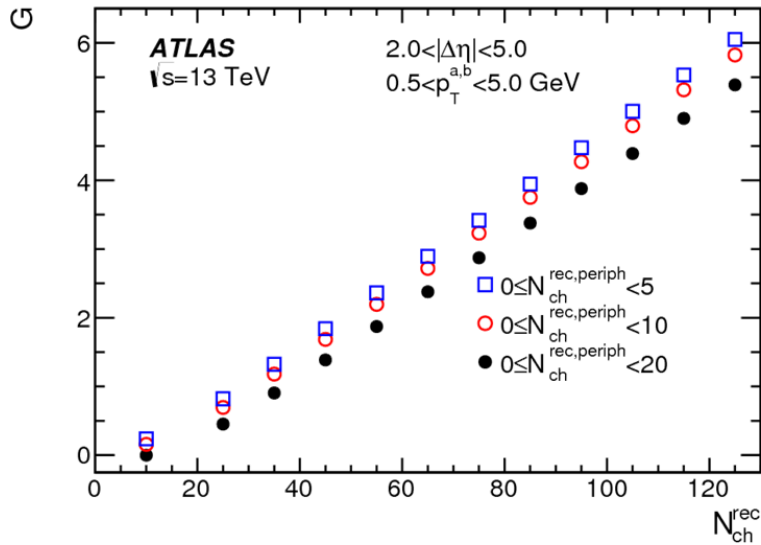
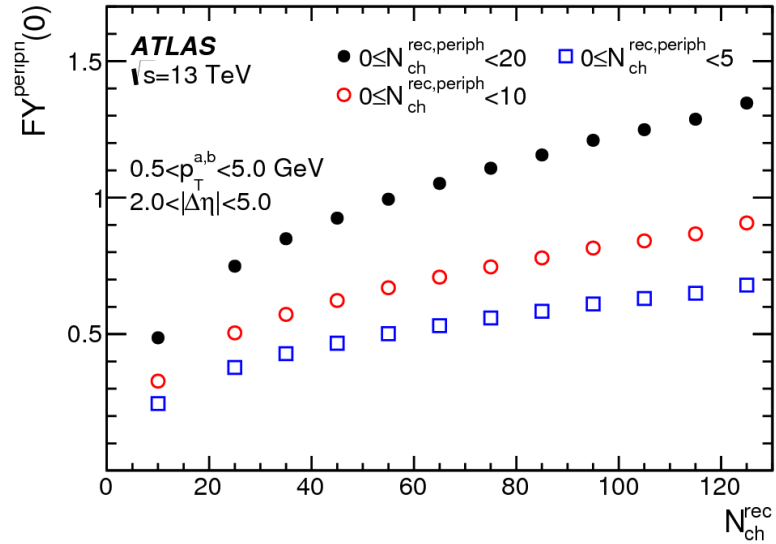
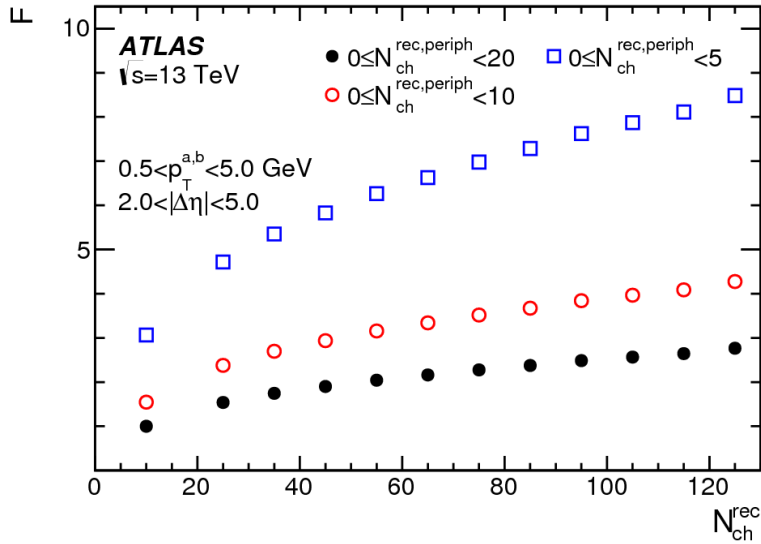


# Template fit at 2.76 TeV

$$Y^{\text{templ}}(\Delta\phi) = Y^{\text{ridge}}(\Delta\phi) + FY^{\text{periph}}(\Delta\phi)$$



# Parameters from template fits



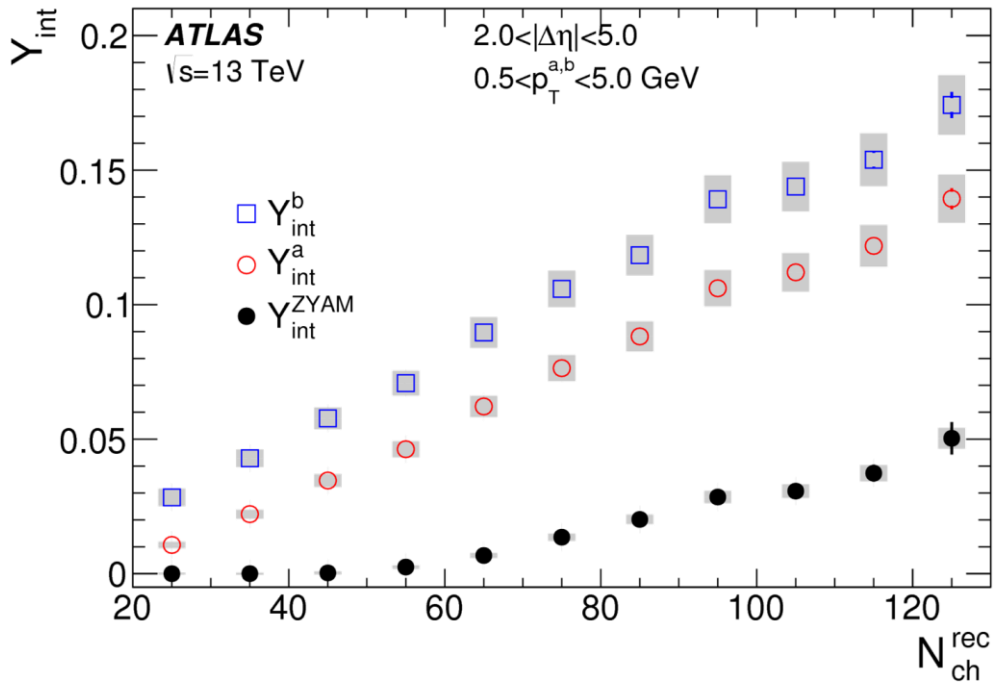
$$Y^{templ}(\Delta\phi) = FY^{periph}(\Delta\phi) + Y^{ridge}(\Delta\phi)$$

$$Y^{ridge}(\Delta\phi) = G(1 + 2v_{2,2} \cos(2\Delta\phi))$$

two free parameters:  $F$  and  $v_{2,2}$

$$G \text{ is fixed by } \int_0^\pi d\Delta\phi Y^{templ} = \int_0^\pi d\Delta\phi Y$$

# $p_T$ dependence of integrated yields



- Results using template fit method from this  $pp$  analysis.
- Results using template fit method from previous  $p+Pb$  analysis.
- Results using ZYAM method.

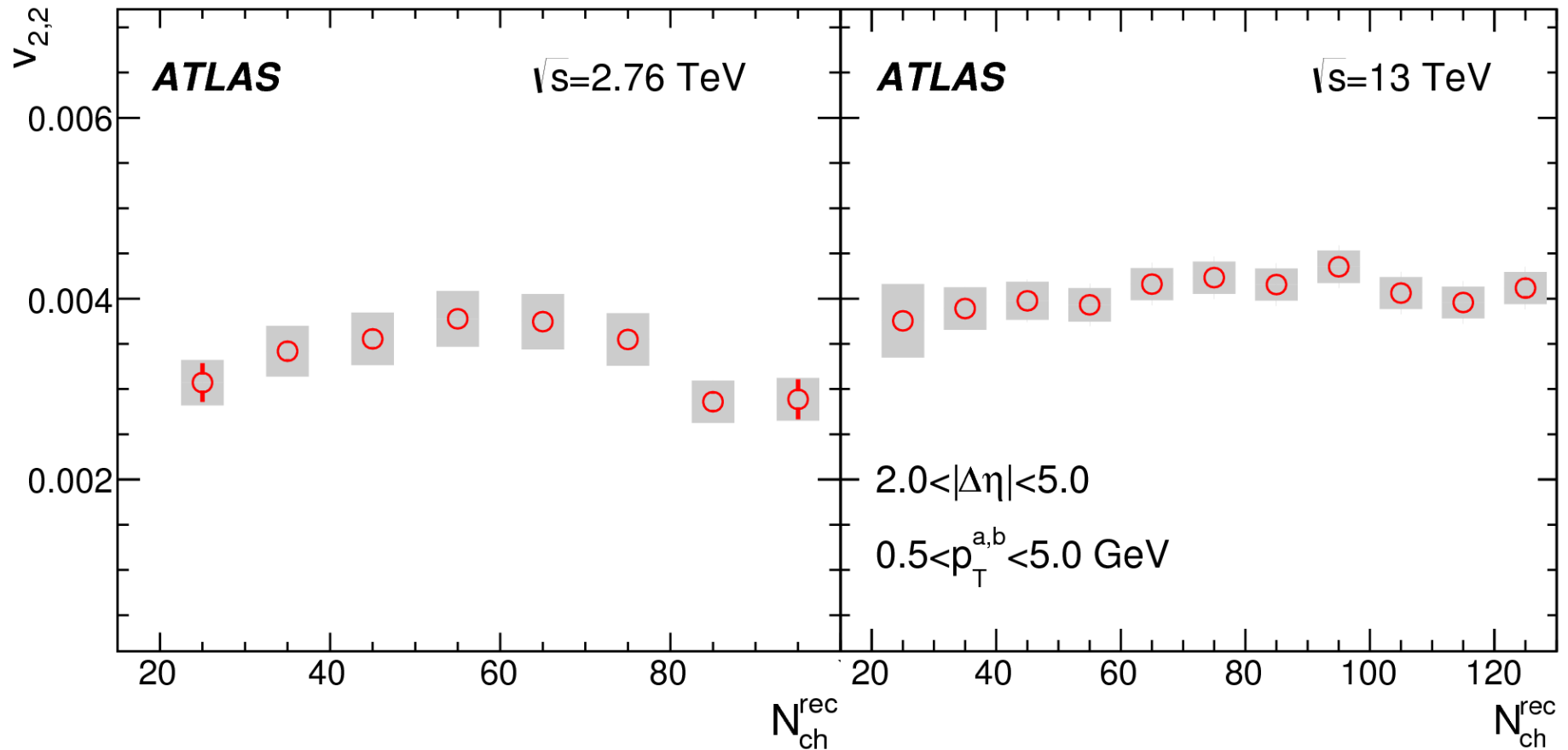
- Due to the modulation of  $v_n$ , estimation of  $b_{ZYAM}$  is biased: ZYAM method underestimates integrated yield;
- Assuming no flow in the peripheral will give a lower bound of  $Y_{int}$ ;
- Assuming same magnitude of flow in the peripheral will give an upper bound of  $Y_{int}$ .

# Details about the template fitting procedure

- If there is  $v_{2,2}$  in peripheral:

$$Y^{\text{peri}}(\Delta\phi) = N_0^{\text{peri}} \left( 1 + 2v_{2,2}^{\text{peri}} \cos(2\Delta\phi) \right) + Y_{\text{jet}}^{\text{peri}}(\Delta\phi)$$

# Energy dependence of $v_{2,2}$



# This is the last slide

